European Journal of Neuroscience, Vol. 21, pp. 3056–3076, 2005

Occipital (V6) and parietal (V6A) areas in the anterior wall of the parieto-occipital sulcus of the macaque: a cytoarchitectonic study

Giuseppe Luppino,[1] Suliann Ben Hamed,[1] Michela Gamberini,[2] Massimo Matelli[1] and Claudio Galletti[2]
[1]Dipartimento di Neuroscienze, Sezione di Fisiologia, Università di Parma, Via Volturno 39, I-43100 Parma, Italy
[2]Dipartimento di Fisiologia umana e generale, Università di Bologna, I-40127 Bologna, Italy

Keywords: dorsal visual stream, extrastriate cortex, superior parietal lobule

Abstract

The anterior wall of the parieto-occipital sulcus (POs) of the macaque monkey, classically considered as part of Brodmann's area 19, contains two functionally distinct areas: a ventral, purely visual area, V6, and a dorsal area, V6A, containing visual neurons and neurons related to the control of arm movements. The aim of this study was to establish whether areas V6 and V6A, so far identified only on a functional basis, have a cytoarchitectonic counterpart. The cytoarchitectonic analysis of 13 hemispheres from ten macaque brains, cut along different planes of section, showed that the anterior wall of the POs contains three distinct areas. One is located in the ventralmost part of the wall, another in the dorsalmost part of the wall, and the third occupies an intermediate position. The ventralmost region displays architectonic features typical of the occipital cytoarchitectonic domain, whereas the two dorsal areas display architectonic features typical of the posterior parietal cortex. Analysis of myeloarchitecture and of the distribution of SMI-32 immunoreactivity confirmed the cytoarchitectonic parcellation. Correlation of cytoarchitectonic maps with functional and hodological data strongly suggests that the ventral region corresponds to area V6, whereas the other two regions correspond to different subsectors of V6A, here named V6Av and V6Ad, respectively. The present data are in line with electrophysiological and hodological data, which suggest that area V6 is a classic extrastriate area, whereas V6A is an area of the posterior parietal cortex. They also suggest that V6A includes two separate cortical subdivisions, a view supported by preliminary functional and hodological data that needs further confirmation.

Introduction

Evidence provided in the early eighties (Covey *et al*., 1982; Gattass *et al*., 1985), based on myeloarchitectural as well as functional criteria, showed the existence of a visual area, termed PO, in the caudalmost part of the superior parietal lobule (SPL), occupying almost entirely the anterior wall of the parieto-occipital sulcus (POs). This finding was in agreement with a number of cytoarchitectonic studies according to which this cortical sector was attributed to the occipital cytoarchitectonic domain (area 19, Brodmann, 1909; area OA, von Bonin & Bailey, 1947; Pandya & Seltzer, 1982).

More recently, area PO was confined to approximately the ventral half of the anterior wall of the POs by Colby *et al*. (1988). At approximately the same time, Zeki (1986) defined a visual area, termed V6, in almost the same location as area PO on the basis of patterns of callosal connections.

In the last decade, the anterior wall of the POs has been the object of extensive electrophysiological studies in awake monkeys (reviewed in Galletti *et al*., 2003), which led to the definition of two functionally distinct areas: a ventral one, termed V6, and a dorsal one, termed V6A. V6 is a retinotopically organized purely visual area, which contains an enlarged representation of the visual field periphery. V6A is a visuomotor area containing visual and nonvisual neurons, some of which are related to the execution of arm movements. These functional properties of V6A do not corroborate the idea that the whole anterior wall of the POs belongs to the occipital cytoarchitectonic domain.

The anatomically defined area PO and the functionally defined area V6, recently, have been considered to correspond to the same cortical area (Lewis & Van Essen, 2000). However, although PO and V6 appear to share similar functional properties, they also show differences in the functional as well as anatomical organization (see Galletti *et al*., 1996, 1999b, 2001; for a thorough discussion on this issue). The major anatomical differences are the smaller cortical extent of V6, with respect to PO, in the anterior wall of the POs, and the different cortical connectivity of PO and V6. Tract tracing studies reported that PO is connected with the posterior parietal areas PGm and 7a (Colby *et al*., 1988), and the dorsal premotor cortex (PMd; Tanné *et al*.; 1995). In contrast, area V6 was reported to be not directly connected to these areas (Galletti *et al*., 2001). These data suggest that PO is not equivalent to V6. Conversely, they suggest that PO includes parts of both V6 and V6A, this latter area being directly connected to PGm, 7a, and PMd (Shipp *et al*., 1998; Marconi *et al*., 2001).

The aim of the present work was to search for possible architectonic counterparts of areas V6 and V6A by using a combined cyto-, immuno-, and myeloarchitectonic approach. We found that V6 and V6A have different architectonic patterns; an occipital pattern for V6 and a parietal pattern for V6A. These results provide architectonic

Correspondence: Professor Giuseppe Luppino, as above.
E-mail: luppino@unipr.it

Received 12 February 2005, revised 11 March 2005, accepted 5 April 2005

doi:10.1111/j.1460-9568.2005.04149.x

criteria useful in defining areas V6 and V6A, so far identified only on the basis of their functional properties (see Galletti *et al*., 1996, 1999a, 1999b). Preliminary data have been presented in abstract form (Ben Hamed *et al*., 2000; Gamberini *et al*., 2002; Luppino *et al*., 2003).

Materials and methods

The cortical architecture of the anterior wall of the POs was analysed in 13 hemispheres from ten macaque monkeys (six *Macaca nemestrina* and for *Macaca fascicularis*), by using a combined cyto-, immuno- and myeloarchitectonic approach. In five of these monkeys (two *Macaca nemestrina* and three *Macaca fascicularis*), where chronic single unit recording and tract tracing experiments were carried out (Galletti *et al*., 1996, 1999a, 1999b; Matelli *et al*., 1998; Luppino *et al*., 2001), the architectonic data were correlated with functional and/or hodological data. The brains used in this study and the type of processing and data analysed in each hemisphere, are summarized in Table 1.

The experimental procedures were approved by the Veterinarian Animal Care and Use Committees of the University of Parma and Bologna, and complied with the European law on the care and use of laboratory animals.

Histological procedures

Each animal used for the architectonic study was anaesthetized with ketamine hydrochloride (15 mg/kg i.m.) followed by an i.v. lethal injection of sodium thiopental and perfused through the left cardiac ventricle with saline, and then with 3.5–4% paraformaldehyde. In all animals but one (Case 1) the perfusion was continued with 5% glycerol. All solutions were prepared in phosphate buffer 0.1 M, pH 7.4. The brains were then exposed, eventually blocked on a stereotaxic apparatus, removed from the skull and photographed. All brains but Case 1 were placed in 10% (three days) and then in 20% (three days) buffered glycerol for cryoprotection. The brain of Case 1 (one hemisphere) was embedded in celloidin and cut parasagittally at 40 μm. All other 12 hemispheres were cut frozen, five coronally, one horizontally and six parasagittally at 60 μm. In all brains, every fifth section was stained with the Nissl method (thionin, 0.1% in 0.1 M acetate buffer pH 3.7) for cytoarchitectonic analysis.

In two animals (Cases 4 and MEF17, three hemispheres, cut parasagittally) every fifth section through the caudal part of the SPL, adjacent to those stained with thionin, was processed for immunohistochemistry by using antibody SMI-32, with a procedure similar to that adopted in previous studies (Geyer *et al*., 2000; Calzavara *et al*., 2005). Immediately after cutting, sections were rinsed in phosphate-buffered saline (PBS) for 10–15 min. Endogenous peroxidase activity was eliminated by incubation in a solution of 0.6% H_2O_2 and 80% methanol for 15 min at room temperature. Sections were rinsed again in PBS for 10–15 min and incubated in a solution of primary antibody (mouse monoclonal SMI-32, dilution 1 : 5000; Sternberger Monoclonals, Baltimore, MD, USA), 0.3% Triton X-100, and 2% normal horse serum in PBS overnight at room temperature. Sections were then processed with the avidin-biotin method by using a Vectastain ABC kit (Vector Laboratories, Burlingame, CA, USA) and 3,3′-diaminobenzidine (DAB) as a chromogen. The reaction product was intensified with cobalt chloride and nickel ammonium sulphate. Steps were performed in the following sequence: PBS for 10–15 min, biotinylated secondary antibody (dilution 1 : 100) and 2% normal horse serum in PBS for 1 h at room temperature, PBS for 10–15 min, ABC solution in PBS for 1 h at room temperature, PBS for 10–15 min, DAB/H_2O_2 solution (50 mg DAB, 2.8 mL of 1% aqueous cobalt chloride solution, 2 mL of 1% aqueous nickel ammonium sulphate solution, 30 μL H_2O_2 30% in 100 mL of 0.1 M phosphate buffer pH 7.4). The duration of the developing reaction in the DAB/H_2O_2 solution was adjusted subjectively, by visual or microscopic inspection of the immunostained sections and was, typically, of approximately 2 min. Sections were rinsed again in PBS for 10–15 min, mounted, dehydrated in graded alcohols, and coverslipped. In order to avoid possible sources of variability among sections from the same case, all sections were processed together in the same solutions.

In three animals (four hemispheres) sections adjacent to those stained with thionin were stained for myelin (Gallyas, 1979).

Data analysis

The architectonic analysis was carried out with a Wild M420 Universal macroscope equipped with an Apozoom objective for low-power observations, and with a Nikon Optiphot-2 and a Zeiss Axioscop 2 microscope for medium- and high-power observations.

In all examined sections, the outer and inner cortical borders and the location of the borders between the various identified cytoarchitectonic areas were plotted with the aid of inductive displacement transducers mounted on the *X*- and *Y*-axes of the microscope stage. The transducer signals were digitized and stored by using software

TABLE 1. Monkey species, type of processing and data analysis

				Data analysis				
Case	Species	Hemisphere	Cut	Nissl stain	Myelin stain	SMI-32 stain	Chronic single unit recordings	Tracer injections
1	*Nemestrina*	Right	Parasagittal	◆				
2	*Fascicularis*	Right	Horizontal	◆				
3	*Nemestrina*	Right	Coronal	◆	◆			
4	*Nemestrina*	Right	Parasagittal	◆	◆	◆		
		Left	Parasagittal	◆	◆	◆		
5	*Nemestrina*	Right	Coronal	◆				
MEF16	*Fascicularis*	Right	Parasagittal	◆			◆	
		Left	Parasagittal	◆			◆	◆
MEF17	*Fascicularis*	Right	Parasagittal	◆			◆	
		Left	Parasagittal	◆	◆	◆	◆	◆
C11 r	*Nemestrina*	Right	Coronal	◆				◆
C13 l	*Fascicularis*	Left	Coronal	◆				◆
C18 l	*Nemestrina*	Left	Coronal	◆				◆

developed in our laboratory that allows the visualization of section outlines, of grey-white matter borders, and of cytoarchitectonic borders.

Data of individual sections from representative hemispheres were then imported into a recently developed 3D reconstruction software (Bettio *et al.*, 2001; Demelio *et al.*, 2001) for reconstructing the anterior wall of the POs and the neighbouring cortical regions, along with the results of the cyto-, immuno- or myeloarchitectonic analysis. The results of this processing allowed us to obtain realistic visualizations of the location and extent of the identified areas, and to compare data obtained from hemispheres cut along different planes of section.

In order to compare present data with previously published functional data (Galletti *et al.*, 1996; 1999a, 1999b), the results from the hemispheres cut parasagittally were also visualized in 2D reconstructions of the caudalmost part of the SPL. The flattened maps were obtained by partial unfolding of the contours of layer 4 from serial sections taken at 300–400-μm intervals, according to the procedure described by Van Essen & Zeki (1978). In this reconstruction, sections were aligned by using two fixed points of reference in the parasagittal sections: (a) the edge between the anterior wall of the POs and the mesial surface of the hemisphere and (b) the border between the anterior wall of the POs and the exposed dorsal surface of the SPL. Two discontinuities were introduced in the reconstruction between adjacent cortical surfaces, corresponding to the maximal curvatures of the cortical mantle, one medially, between the dorsal and mesial surfaces, the other laterally, between the dorsal surface and the medial bank of the intraparietal sulcus (for more details, see Galletti *et al.*, 1996).

Correlation with functional and hodological data

The possible correlation of architectonic patterns with functional data was examined by analysing the cytoarchitecture of the anterior wall of the POs in two animals (MEF16 and MEF17) in which areas V6 and V6A were functionally defined in chronic single unit experiments carried out on the awake animal. In each histological section, electrode trajectories were reconstructed on the basis of electrolytic lesions, recording coordinates, and other landmarks described in detail in Galletti *et al.* (1999b). The sites of recording along each penetration were attributed to the functional areas V6 and V6A on the basis of the functional criteria described in Galletti *et al.* (1996, 1999a, 1999b). The results of the cytoarchitectonic analysis (borders between different cytoarchitectonic patterns) were superimposed in the same section to the electrode tracts and recording sites. The combined cytoarchitectonic and electrophysiological data were then displayed on 2D reconstructions of the anterior wall of the POs carried out by the above-mentioned procedure.

Architectonic data were also correlated with previous hodological data on the cortical connections of area V6 (Galletti *et al.*, 2001), and on the frontal projections from the caudal part of the SPL (Matelli *et al.*, 1998). To this purpose, we re-examined data from two macaque monkeys (MEF16 and MEF17) in which WGA-HRP was injected into area V6, functionally identified in the awake animal (for further details, see Galletti *et al.*, 2001), and from three macaque monkeys (Cases 11r, 13 l, and 18 l) in which neural tracers (Fast blue, Diamidino Yellow, Gold-conjugated cholera toxin B subunit) were injected into areas F2 and F7 (for further details see Matelli *et al.*, 1998 and Luppino *et al.*, 2001). The cytoarchitecture of the anterior wall of the POs was analysed in parasagittal (MEF16 and MEF17) or in coronal (Cases 11r, 13 l, and 18 l) sections through the caudal part of the SPL. Cytoarchitectonic borders were then superimposed to the distribution of retrogradely labelled neurons in each section, and 2D/3D reconstructions of combined architectonic and hodological data were finally obtained.

Photographic presentation

Photomicrographs shown in the present study were obtained by capturing images directly from the sections with a digital camera attached to the macroscope or to the microscope. Individual images were then imported in Adobe Photoshop in which they could be processed, eventually assembled into digital montages and reduced to the final enlargement. As in classical photographic procedures, image processing in several cases required lighting, contrast, brightness or sharpness adjustments. Data were never altered by this electronic processing.

Results

Cytoarchitecture of the anterior wall of the POs

Overview of architectonic patterns

The results of the present study are largely based on the analysis of parasagittal sections, which, especially when passing through the middle of the SPL, offer a complete view of the anterior wall of the POs, the cortical mantle in these sections being cut almost perpendicularly to the cortical surface.

The upper part of Fig. 1 shows a low-power photomicrograph of a parasagittal section through the anterior wall of the POs from Case 1. A high-power analysis of the histological material showed the presence of several cytoarchitectonic subdivisions in this cortical sector. The fundus of the POs was occupied by a cortical region showing a cytoarchitectonic organization typical of occipital areas. Given its anatomical location and its general architectural features, we considered it to be area V3. At the dorsal limit of the anterior bank of POs, the cortex extending upon the caudalmost part of the exposed surface of the SPL showed the typical organization of parietal areas. Its location and cytoarchitectonic organization very likely corresponds to area PEc of Pandya & Seltzer (1982). The cortex in between areas V3 and PEc, occupying the entire anterior bank of POs, clearly showed two major cytoarchitectonic subdivisions, marked by black arrowheads in the figure. The ventral region, bordering V3, showed an occipital pattern, the dorsal region, bordering PEc, a parietal pattern. On the basis of correlation with functional and connectional data (see below), these two cytoarchitectonic subdivisions are suggested to

FIG. 1. Cytoarchitectonic subdivision of the anterior wall of the parieto-occipital sulcus. (Top) Low-power photomicrograph of a Nissl-stained parasagittal section, centred on the anterior wall of the POs. In the photomicrograph, dorsal is on the right and rostral is down. Scale bar, 1 mm. Arrows mark the borders between cytoarchitectonic areas. Dashed box on the section drawing indicates the location of the photomicrograph shown on the top, shaded boxes indicate the location of the higher magnification views. Dashed line on the drawing of the dorsal view of the hemisphere on the left, indicates the level at which the section was taken. (Middle right and bottom) Higher magnification views from the same section of cytoarchitectonic areas V3, V6, V6Av, V6Ad and PEc. Scale bar (shown in PEc), 200 μm. AS, superior arcuate sulcus; C, central sulcus; c, caudal; Cal, calcarine fissure; d, dorsal; IP, intraparietal sulcus; L, lateral fissure; Lu, lunate sulcus; POm, medial parieto-occipital sulcus; POs, parieto-occipital sulcus; r, rostral; ST, superior temporal sulcus; v, ventral.

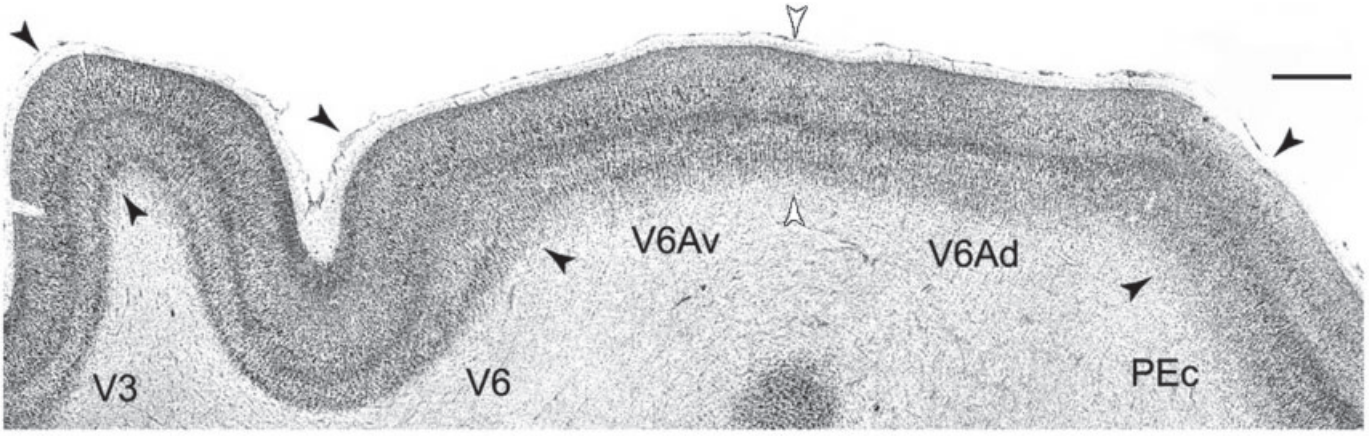
V6Av
V6Ad
V3
V6
PEc

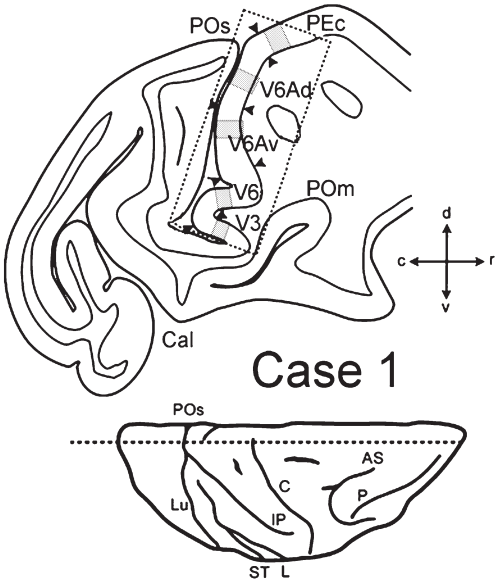
POs
PEc
V6Ad
V6Av
V6
POm
V3
d
c
r
v
Cal
Case 1
POs
AS
C
P
Lu
IP
ST
L

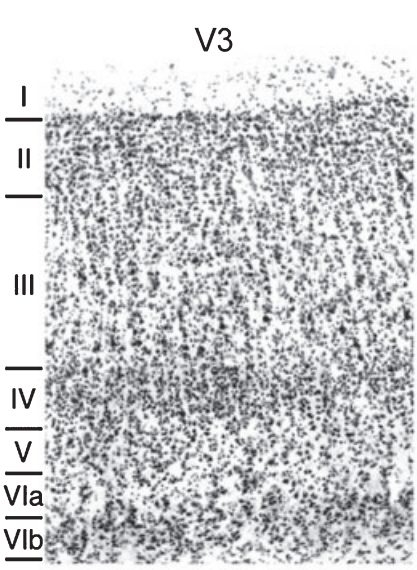
V3
I
II
III
IV
V
VIa
VIb

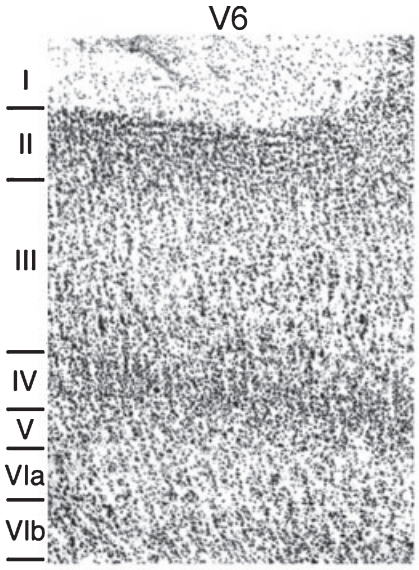
V6
I
II
III
IV
V
VIa
VIb

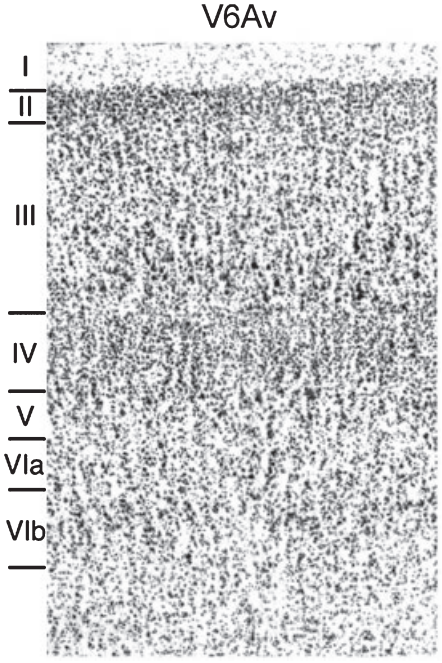
V6Av
I
II
III
IV
V
VIa
VIb

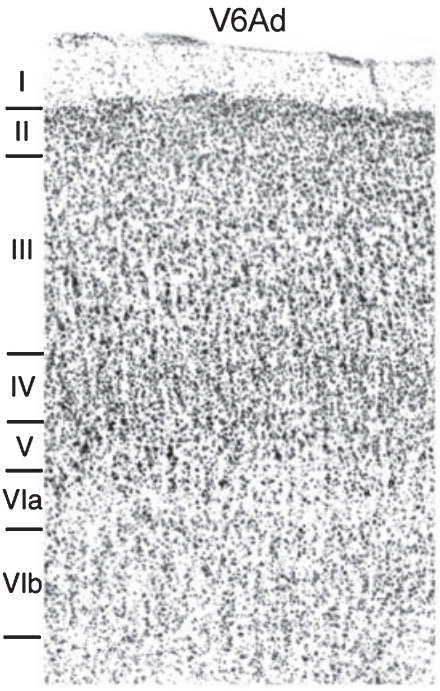
V6Ad
I
II
III
IV
V
VIa
VIb

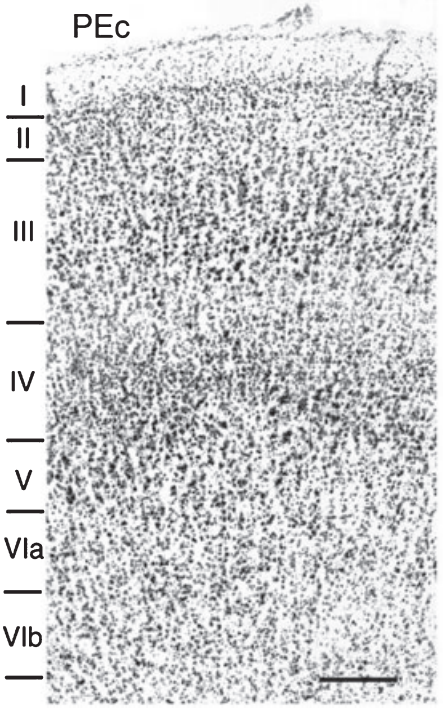
PEc
I
II
III
IV
V
VIa
VIb

represent the architectonic counterpart of the functional areas V6 and V6A, respectively. Therefore, from now on in this paper we will refer to these cortical regions as V6 and V6A.

As shown in Fig. 1, area V6 occupies the ventral third of the anterior wall of POs, and area V6A the dorsal two-thirds. Higher-power analysis of the histological material showed also that area V6A is architectonically a nonhomogeneous field. It can be subdivided into a ventral and a dorsal part, which will be referred to as V6Av and V6Ad. The border between these two V6A subdivisions is marked by empty arrowheads in the upper part of Fig. 1.

Preliminary remarks to the detailed description of the architectonic features of these areas are, firstly, that architectonic features typically do not change abruptly from one area to another, but transitions can be gradual, usually in the range of less than 1 mm. Accordingly, areal borders shown in the photomicrographs represent the intermediate points of the identified transitions. Secondly, some general architectonic features, e.g. cell density and size, often show interindividual variability due, in part, to technical reasons, such as, for example, differences in shrinkage due to histological processing. Accordingly, areal identification mostly based on absolute changes in individual histological elements, very often results in a high degree of variability in the obtained architectonic parcellations, which is a strong argument against the cytoarchitectonic approach (see Matelli & Luppino, 2004). For this reason, the goal in this study was to focus on a combination of multiple relative cytoarchitectonic changes, within individual cases, in single layer individual histological elements features, which could be reliably and consistently observed across different cases. Moreover, uncertainties attributed to distortion of architectonic features due to planes of section not perpendicular to the cortical surface were in part eliminated by using material from different planes of section. In this way, we identified a set of architectonic criteria, effective in characterizing the areas identified in this study across cases, despite interindividual variability, and in obtaining remarkably constant architectonic maps in different brains.

Detailed description of architectonic patterns

Higher magnification views of the three identified cytoarchitectonic areas V6, V6Av, and V6Ad, as well as of the adjacent ventral area V3 and dorsal area PEc, are shown in the middle and lower parts of Fig. 1.

Cytoarchitectonic features common to both V6 and V3, which characterize them as occipital areas, are a thick, homogeneous layer IV with densely packed granular cells, a light layer V, populated by small pyramids, and a clear subdivision of layer VI into two sublayers, with a very dense layer VIb, sharply delimited with respect to layer VIa and the white matter.

Cytoarchitectonic features common to V6Av, V6Ad and PEc, which characterize these areas as homotypical parietal areas, are well-developed layers III and V, with a relatively large number of medium-sized pyramids, a relatively dense layer IV, in which the upper part appears to be somewhat less dense than the lower one, and a layer VI with a poorly evident subdivision into sublayers and a relatively blurred border against the white matter.

In spite of many evident similarities, several cytoarchitectural differences characterize the two occipital areas V3 and V6 (Fig. 1, middle part). V6 shows an evident layer II with densely packed small cells and a dense layer III with a relatively small amount of medium-sized pyramids in its lowest part. In addition, a radial cellular organization is well evident in layer VI, with thin vertical columns of cells very close to each other. In V3, layer II is less sharply delineated and layer III displays a more evident size gradient, with a relatively large amount of medium-sized pyramids in its lower half. Furthermore, with respect to V6, the radial cellular organization is less evident in layer VI, and layer VIb is more sharply defined, because of the presence of relatively large cells. The presence of larger cells and a coarser radial organization, especially in layer III, give to V3, even at low-power views, the appearance of a coarser cellular texture with respect to V6.

Several cytoarchitectural features also differentiate the three parietal areas, V6Av, V6Ad and PEc from each other (Fig. 1, lower part). Area PEc is characterized by the presence of a very clear size gradient in layer III, which is densely populated by medium-sized pyramids in its lower part, and by a dense layer V with a high number of relatively large pyramids. These cytoarchitectural features are in accord with those described for area PEc by Pandya & Seltzer (1982). With respect to area PEc, V6A, as a whole, is characterized by a much less pronounced size gradient in layer III and by the presence of smaller and fewer pyramids in layer V. V6A, however, appears to be nonhomogeneous in its dorso-ventral extent. In the ventral part of V6A, here defined as V6Av, layer II is well delineated and layer III displays a size gradient with relatively larger pyramids in its lower part, evident even at a low-power view in Fig. 1 (upper part). Layer V is relatively well developed, and populated mostly by medium-sized pyramids. In layer VI, two sublayers can be roughly detected, but the border of layer VI with the white matter is blurred, in strong contrast with that of V6. The dorsal part of V6A, here defined as V6Ad, is characterized by a relatively poorly defined layer II and a homogeneous layer III. The overall cell density is lower than in V6Av in both layers II and III, and only a few, medium-sized pyramids are present in the lower part of layer III. Layer V, richer than in V6Av, also contains scattered relatively larger pyramids. Layer VI is more homogeneous and its border with the white matter less evident. The subdivision of V6A into two similar, but distinct, subfields, though based on relatively subtle cytoarchitectonic criteria, was constantly observed across different sections and cases and, as it will be shown below, also appears to be supported by immuno- and myeloarchitectonic data.

Figure 2 shows higher magnification views of the major cytoarchitectonic features that distinguish the occipital area V6 from the parietal area V6Av. Layer III in V6 is quite homogeneous, with few medium-sized pyramids in the lowest part, whereas in V6Av the pyramids progressively increase in size from the upper to the lower part of this layer. Layer IV in V6 contains very densely packed granular cells, whereas it is markedly less densely populated in V6Av. Layer V in V6 is relatively thin and populated by sparse, small pyramids, whereas it is more developed and rich in medium-sized pyramids in V6Av. Occasionally, also relatively large pyramids could be observed. Finally, layer VI is denser in V6, with respect to V6Av and, in particular, layer VIb is more sharply delimited.

The medial and lateral borders of V6 and V6A were hardly recognized in parasagittal sections, as in the medial and lateral parts of the SPL the cortex is cut almost tangentially by a parasagittal plane of section. On the contrary, they were optimally defined in sections cut horizontally. Figure 3 shows two horizontal sections through the caudal pole of the SPL, taken at different dorso-ventral levels, from Case 2. Arrowheads on sections mark the medial and lateral borders of areas V6, V6Av, and V6Ad. Enlarged views taken from these two sections are shown in Fig. 4. Figure 3 shows that V6 is almost completely confined to the anterior wall of the POs, whereas V6Ad and V6Av extend more rostrally, in the medial and lateral aspects of caudal SPL. In addition, V6Av also extends ventrally, surrounding anteriorly area V6.

On the medial and lateral aspects of the SPL, V6Ad and V6Av border cytoarchitectonically different cortical sectors. On the medial surface of the hemisphere, they border a cortical region characterized

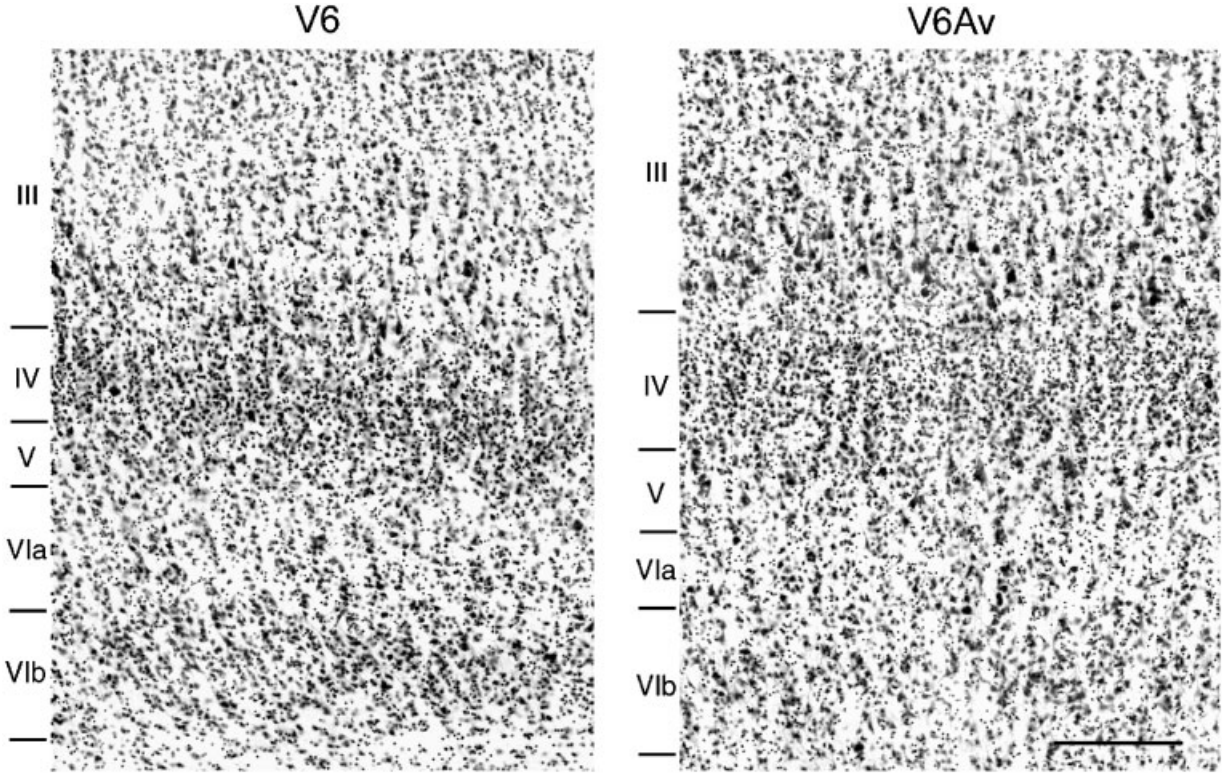

FIG. 2. High power photomicrographs of representative fields of cytoarchitectonic areas V6 and V6Av from the same section of Fig. 1. Scale bar (shown in V6Av), 200 μm.

by a thick and homogeneous layer III, a layer V populated by many small pyramids, and a relatively dark layer VI (see Fig. 4). This cortical sector corresponds to area PGm of Pandya & Seltzer (1982). The increase in thickness of layer III and the presence of a layer V densely populated by small pyramids in PGm represent the most reliable cytoarchitectural criteria for setting the medial border of both V6Ad and V6Av. In the medial bank of the intraparietal sulcus, the cortical region rostral to V6Ad and V6Av displays a clear increase in the size and density of medium-sized pyramids in layers III and V (Fig. 4). These features represent reliable cytoarchitectonic criteria for setting the lateral border of V6Ad and V6Av with a cortical sector that might correspond to the so-called medial intraparietal area (MIP), till now mostly defined on the basis of functional and connectional data (Colby *et al*., 1988; Colby & Duhamel, 1991). As described above, the presence of a less dense and more homogeneous layer III, without any clear size gradient, a richer layer V and a more homogeneous layer VI, less sharply defined against the white matter, characterize V6Ad with respect to V6Av (Fig. 4).

Several cases analysed in this study were cut in the coronal plane, which is the most widely used plane of section. In coronal sections, it is possible to identify both V6 and V6A on the mesial surface of the hemisphere and on the medial bank of the intraparietal sulcus. Figure 5 shows on the left a low-power view of a coronal section from Case 3 through the caudalmost part of the SPL. The location of V6 and V6A on the mesial surface of the hemisphere, along with higher magnification views of V6, V6Av and V6Ad, are shown in the figure. At this level on the mesial surface of the hemisphere, V6 is almost completely confined to the upper bank of the medial parieto-occipital sulcus. The V6/V6A border is sharply defined, even at low-power view, as in Fig. 1, in both the mesial surface of the hemisphere and in the medial bank of the intraparietal sulcus, due to the marked decrease in density in layer IV at the transition from V6 to V6A. Here again, it is evident that the architectonic pattern within V6A is not homogeneous. In V6Av, with respect to V6Ad, layer III is denser and displays a more evident size gradient, layer V less rich and the differentiation of layer VI into two sublayers is more evident, even at low-power view.

One problem encountered with coronal sections was the difficulty in defining V6 and V6A on the anterior wall of the POs, this cortical sector being placed almost tangentially to the plane of section. The analysis of parasagittal and horizontal sections, however, clearly showed that the borders of V6 and V6A run almost horizontally on the wall of POs. Therefore, the location of V6 and V6A borders on the anterior wall of the POs in cases cut in coronal sections can be, with a very high degree of approximation, extrapolated on the basis of their location on the mesial cortical surface and on the medial bank of the intraparietal sulcus.

Immuno- and myeloarchitecture of the anterior wall of the POs

Sections from three hemispheres immunoreacted for the visualization of the distribution of SMI-32 immunoreactivity, were also used in this study to validate the cytoarchitectonic definition of V6, V6Av and V6Ad with an independent architectonic approach.

SMI-32 is a monoclonal antibody directed against nonphosphorylated neurofilament proteins, which reveals subpopulations of pyramidal neurons in the primate neocortex (Campbell & Morrison, 1989) and has proved to be an effective architectonic tool in the macaque for the delineation of occipito-parietal (e.g. Hof & Morrison, 1995), temporal (Cusick *et al*., 1995), agranular frontal (e.g. Geyer *et al*., 2000), cingulate (Nimchinsky *et al*., 1996) and prefrontal (Carmichael & Price, 1994) areas.

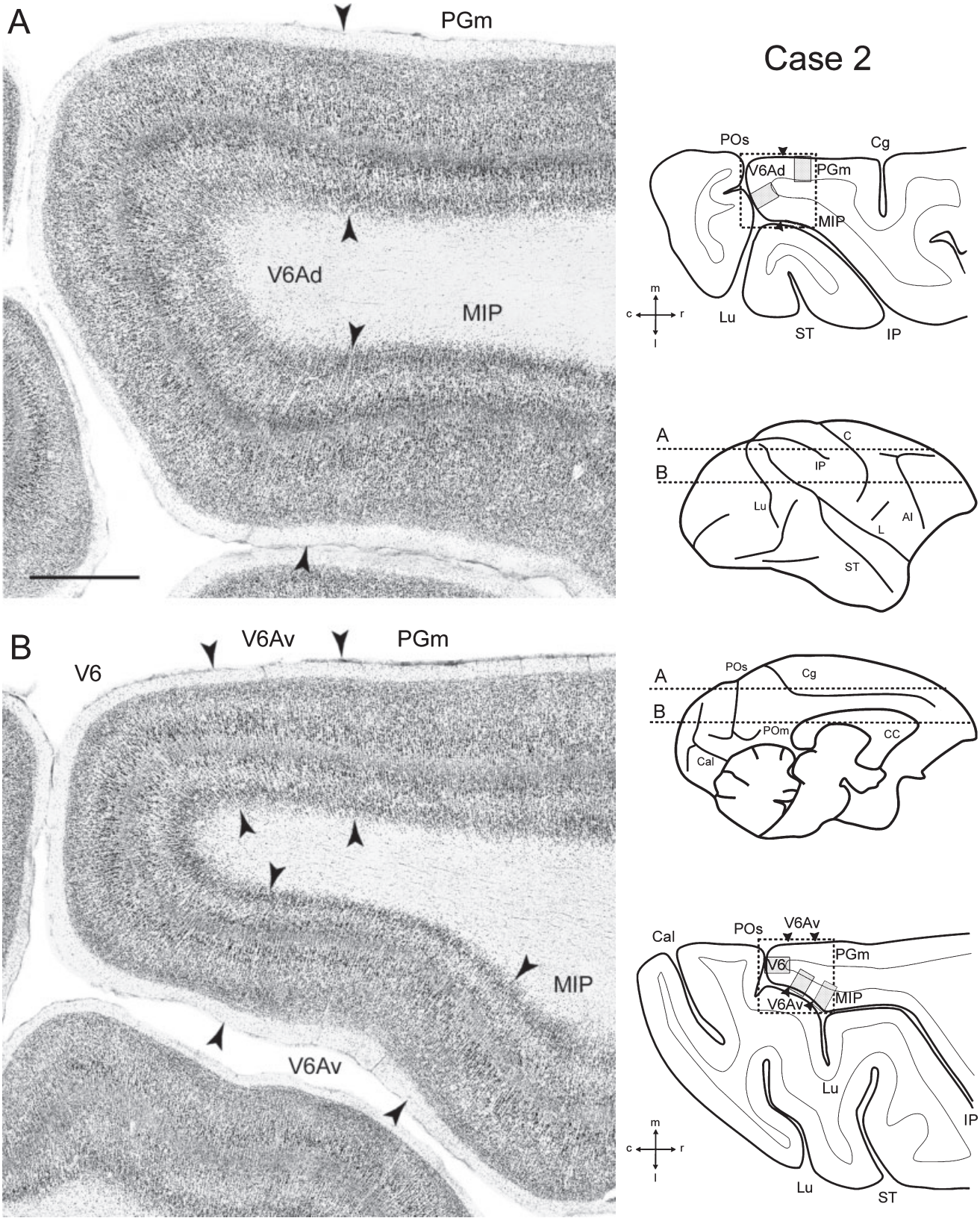

FIG. 3. Cytoarchitectonic subdivision of the posterior part of the superior parietal lobule. (A and B) Low-power photomicrographs of two Nissl-stained, horizontal sections showing the extent of the parieto-occipital areas on the anterior wall of the POs, the mesial cortical surface and the medial bank of the intraparietal sulcus. Mesial is up and rostral is on the right. Drawings of the lateral and mesial views of the hemisphere on the right indicate the levels at which the sections were taken. Dashed boxes on the sections drawings indicate the location of the two photomicrographs shown on the left, shaded boxes indicate the location of the photomicrographs shown in Fig. 4. Scale bar (shown in A), 1 mm. AI, inferior arcuate sulcus; CC, corpus callosum; Cg, cingulate sulcus; m, mesial; l, lateral. Other conventions and abbreviations as in Fig. 1.

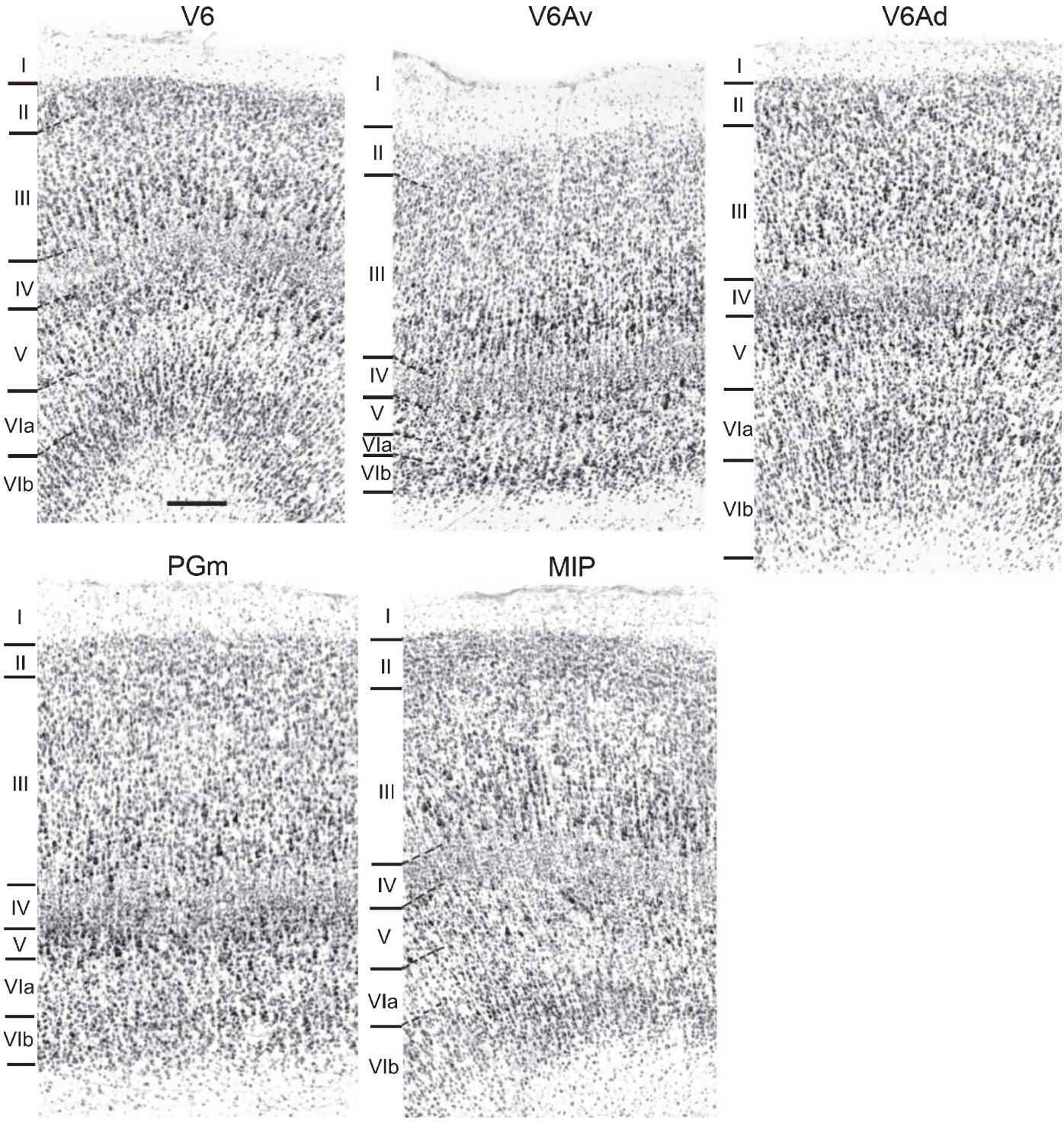

FIG. 4. Photomicrographs of representative fields of cytoarchitectonic areas V6, V6Av, V6Ad, PGm and MIP, taken from the sections shown in Fig. 3. The locations of photomicrographs are indicated by shaded boxes in the section drawings shown in Fig. 3. Scale bar (shown in V6), 200 μm.

We found SMI-32 immunoreactivity very helpful also for the definition of areas V6 and V6A and for characterizing them as an occipital and a parietal area, respectively. Figure 6 shows a low-power view of a parasagittal section from Case MEF17, immunoprocessed for SMI-32 immunoreactivity, and higher magnification views of selected fields from the same section, in which borders of layers III, IV and V, defined in adjacent Nissl-stained sections, are also indicated. V6, as well as other occipital extrastriate areas, displays a relatively high immunoreactivity in lower layer III, with dense, relatively small immunopositive pyramids concentrated in lower layer III and dense immunopositive apical dendrites, which in many cases ascend to more superficial layers. In contrast, layer V, which is usually very rich in positive pyramidal cell bodies in parietal, agranular frontal and cingulate areas, presents only very few, small and weakly positive

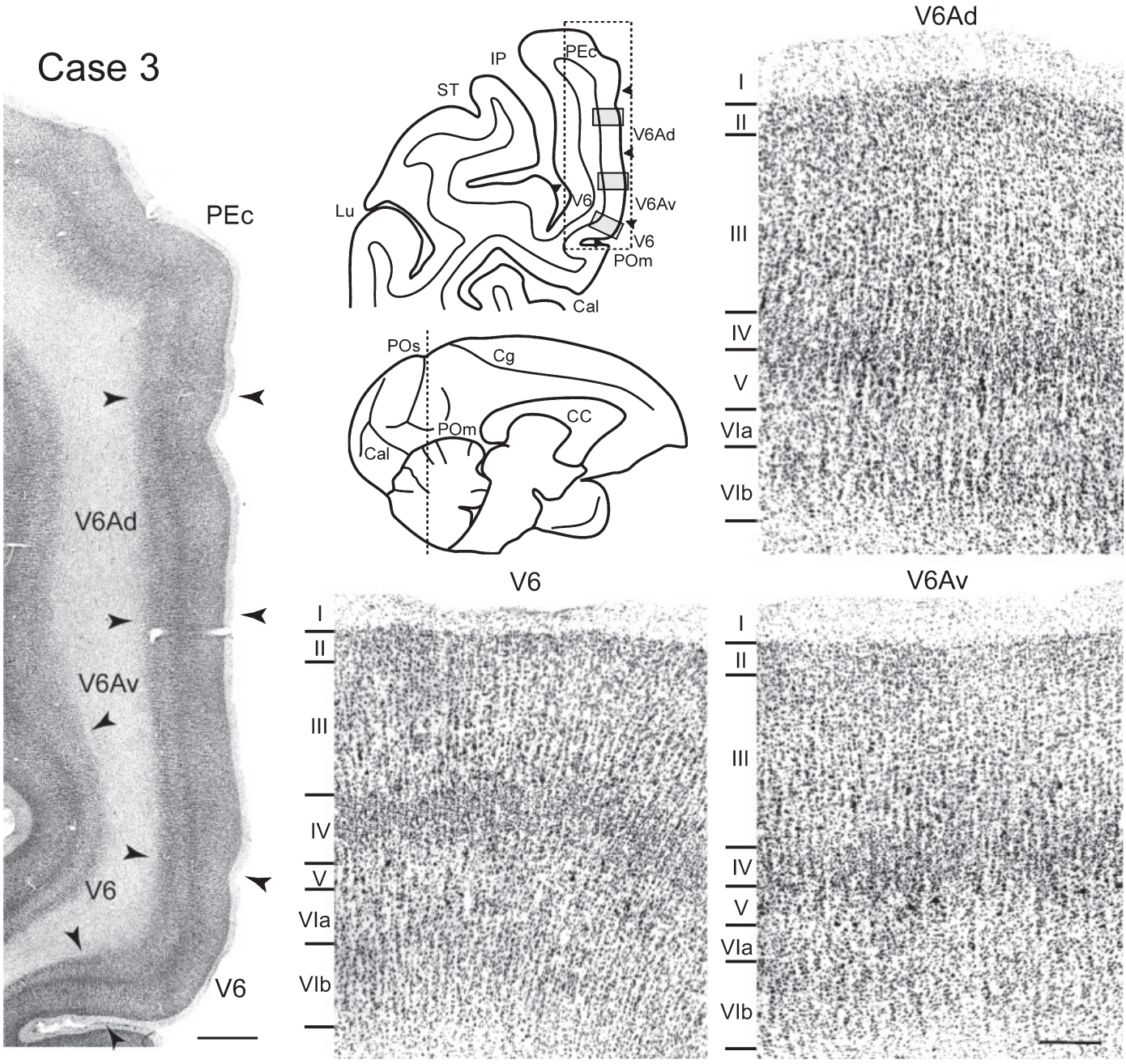

FIG. 5. Cytoarchitectonic subdivision of the caudal precuneate cortex. (Left) Low-power photomicrograph of a Nissl-stained coronal section, showing the cytoarchitecture of the mesial wall of the hemisphere close to the junction with the anterior wall of the POs. Dorsal is up and mesial is on the right. Scale bar, 1 mm. (Center) Drawing of the mesial view of the hemisphere indicating the level at which the section was taken. Dashed box on the section drawing indicates the location of the photomicrograph shown on the left. (Right and bottom) Higher magnification views of representative fields, from the same section, of areas V6, V6Av and V6Ad. The location of the photomicrographs is indicated by shaded boxes in the section drawing. Scale bar (shown in V6Av), 200 μm. Conventions and abbreviations as in Figs 1 and 3.

pyramids in area V6 and in other occipital areas. The distribution of SMI 32 immunoreactivity is markedly different in V6A. In layer III, the overall staining intensity is clearly lower than in V6, because of a more loose arrangement of layer IIIc positive pyramids, which are numerous and relatively larger than in V6, and because of a much smaller amount of positive apical dendrites, mostly confined to layer IIIc. Furthermore, many relatively large immunostained pyramids are present in layer V. The decrease in the overall staining intensity in layer III and the presence of many positive cell bodies in layer V are two criteria that allowed us to reliably characterize the transition from area V6 to area V6A. The transition was in exact correspondence with the cytoarchitectonic border between the two areas.

As in Nissl-stained material, some minor, but constant architectural differences were found between the ventral and dorsal parts of area V6A, the most striking one being the presence in V6Ad of positive cell bodies, in both layers III and V, larger and more numerous than in V6Av. The transition between these two V6A immunoarchitectonic subfields was found in close correspondence (within the range of less

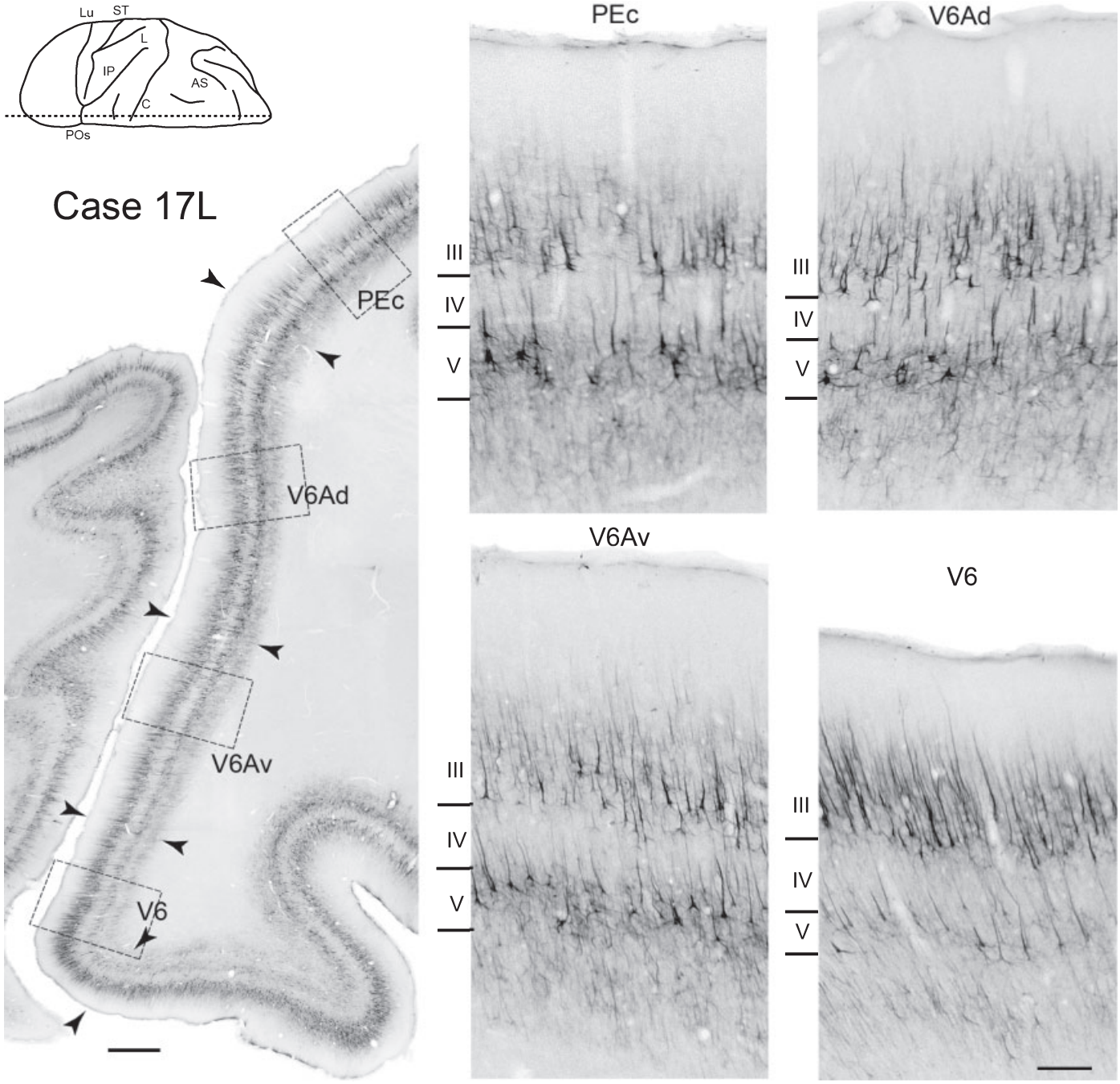

FIG. 6. SMI-32 immunoarchitecture of the anterior wall of the POs. (Left) Low-power photomicrograph of an immunoprocessed parasagittal section, showing the distribution of SMI-32 immunoreactivity in the anterior wall of the POs. Dorsal is up and rostral is on the right. Dashed boxes on the low-power photomicrograph indicate the location of the higher magnification views. Scale bar, 1 mm. Dashed line on the drawing of the dorsal view of the hemisphere on the top, indicates the level at which the section was taken. (Right) Higher magnification views from the same section showing laminar patterns of SMI-32 immunoreactivity distribution in areas V6, V6Av, V6Ad and PEc. Borders between layers are reported from an adjacent Nissl-stained section. Scale bar (shown in V6), 200 μm. Conventions and abbreviations as in Figs 1 and 3.

than 500 μm) with that observed in adjacent Nissl-stained sections. Finally, area PEc was characterized by a further decrease in the overall number of immunopositive pyramids in both layers III and V, which, however, were considerably larger than in V6Ad.

The above described immunoarchitectonic features of V6, V6Av, and V6Ad, were constantly observed across different sections and hemispheres.

In order to compare the location and extent of the cytoarchitectonic areas defined in this study with the myeloarchitectonic subdivision of the caudal SPL proposed by other authors (Colby *et al*., 1988), sections cut frozen in coronal or parasagittal planes were also stained for myelin. In agreement with the common histological experience, we found that very often the quality of the staining varied from section to section, or even in the same section, mainly because of differences in

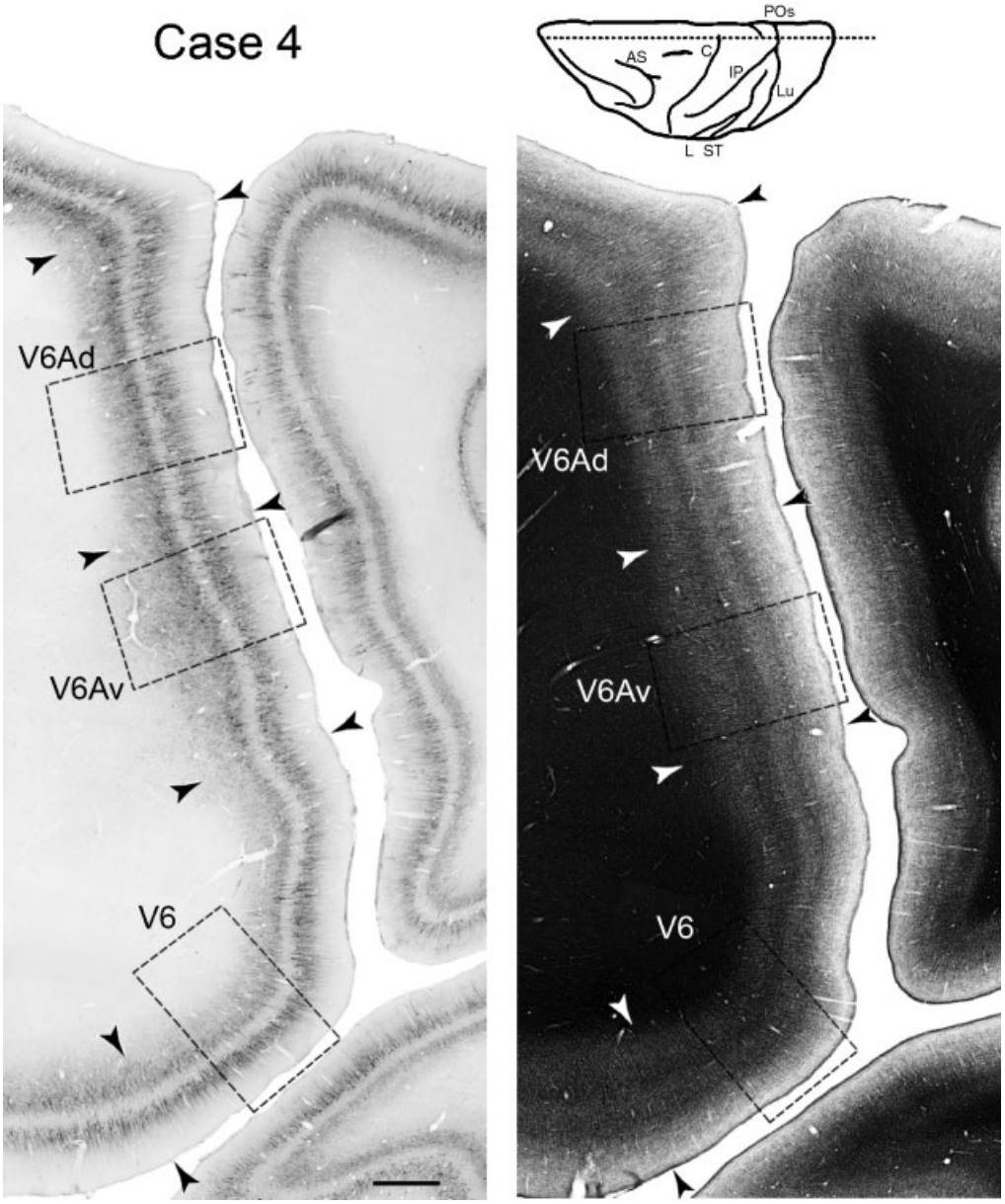

FIG. 7. SMI-32 immunoarchitecture and myeloarchitecture of the anterior wall of the POs. Low power photomicrographs of adjacent parasagittal sections immunoprocessed for SMI-32 immunoreactivity (left) or stained for myelin (right). Dorsal is up and rostral is on the left. Dashed boxes on the photomicrographs indicate the location of the higher magnification views shown in Fig. 8. Dashed line on the drawing of the dorsal view of the hemisphere on the top, indicates the level at which the section was taken. Scale bar, 1 mm. Conventions and abbreviations as in Figs 1 and 3.

the density of silver impregnation. Given the existence of these technical problems, we based our analysis only on the myeloarchitectural patterns that were reliably observed across different sections. According to this criterion, three main myeloarchitectural sectors were identified along the dorso-ventral extent of the caudalmost part of SPL. Correlation with adjacent Nissl-stained sections and, when possible, with SMI-32 processed material, showed that these three sectors correspond quite well to the cytoarchitectonic areas V6, V6Av and V6Ad.

Photomicrographs from representative parasagittal and coronal myelin-stained sections are shown in Figs 7 and 8 (Case 4, section adjacent to Nissl and SMI-32 immunoreacted sections) and in Fig. 9 (Case 3, section adjacent to the Nissl-stained one shown in Fig. 5), respectively. Low-power views in Fig. 7 (right) and Fig. 9 (left) show

FIG. 8. SMI-32 immunoarchitecture and myeloarchitecture of the anterior wall of the POs. Higher magnification views of representative fields from the SMI-32 immunoprocessed (left) and from the myelin-stained (middle) sections shown in Fig. 7 (and there indicated by shaded boxes), centred on V6 (bottom), V6Av (middle) and V6Ad (top). The same fields from an adjacent Nissl-stained section are shown on the right. Scale bar (shown in the top left photomicrograph), 200 μm. iB, inner stria of Baillarger; oB, outer stria of Baillarger. Conventions as in Fig. 6.

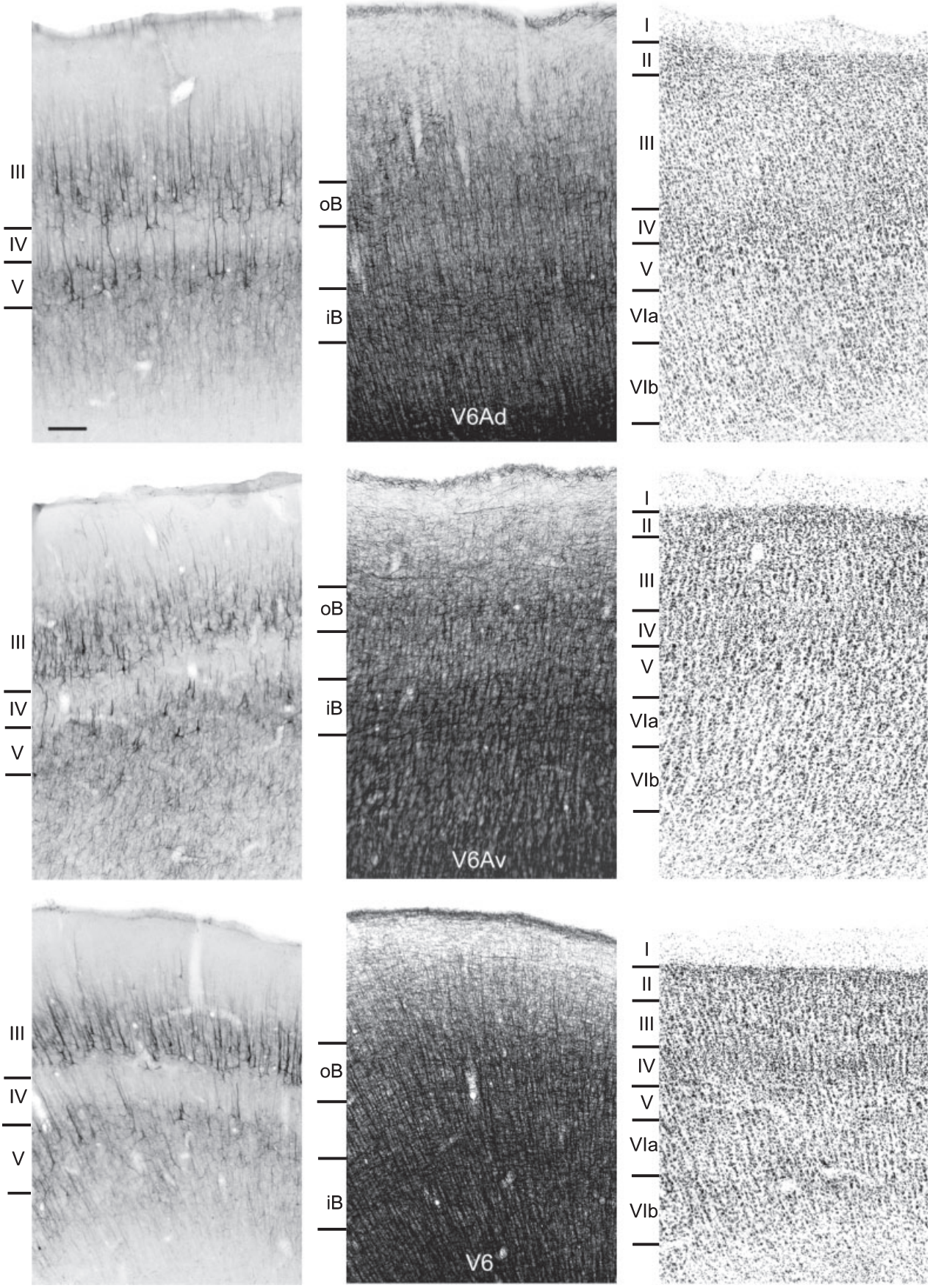
III
IV
V
oB
iB
V6Ad
I
II
III
IV
V
VIa
VIb
III
IV
V
oB
iB
V6Av
I
II
III
IV
V
VIa
VIb
III
IV
V
oB
iB
V6
I
II
III
IV
V
VIa
VIb

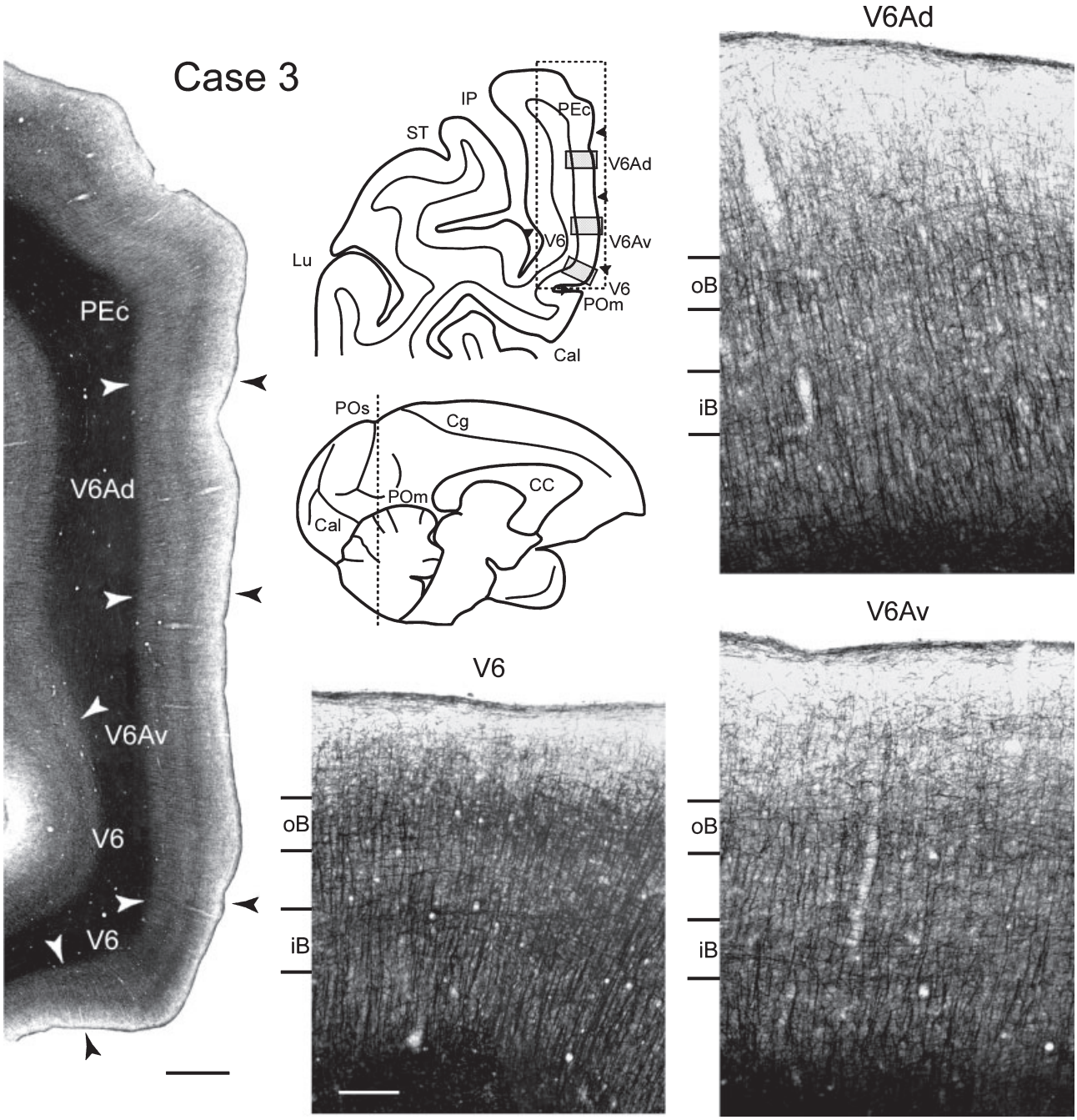

FIG. 9. Myeloarchitectonic subdivision of the caudal precuneate cortex. (Left) Low-power photomicrograph of a coronal section stained for myelinated fibers, adjacent to the section shown in Fig. 5, showing the myeloarchitecture of the mesial wall of the hemisphere at the junction with the anterior wall of the POs. Dorsal is up and mesial is on the right. Scale bar, 1 mm. (Center) Drawing of the mesial view of the hemisphere indicating the level at which the section was taken. Dashed box on the section drawing indicates the location of the photomicrograph shown on the left. (Right and bottom) Higher power photomicrographs of representative fields from the same section, showing the myeloarchitecture of areas V6, V6Av and V6Ad. The location of the photomicrographs is indicated by shaded boxes in the section drawing. Scale bar (shown in V6), 200 μm. Conventions and abbreviations as in Figs 1, 3 and 8.

that, moving ventro-dorsally, a marked decrease in the myelin content was observed corresponding to the cyto- or immunoarchitectonic border between V6 and V6A. A further, though less pronounced, decrease was observed in correspondence of the V6Av/V6Ad border. Higher magnification views in Figs 8 and 9 show that V6 is a highly myelinated area. Vertical bundles of fibers are relatively thick, dense and clearly visible, even above the outer band of Baillarger. Both inner and outer Baillarger bands are very evident and densely impregnated. V6Av is well myelinated, though less than V6. Vertical bundles of thick fibers are sparser and tend to stop at the level of the outer band of Baillarger. Both Baillarger bands are clearly visible, but are less densely impregnated than in V6 (in particular the outer band). In V6Ad, vertical bundles of fibers are sparser and the Baillarger bands are less densely impregnated than in V6Av.

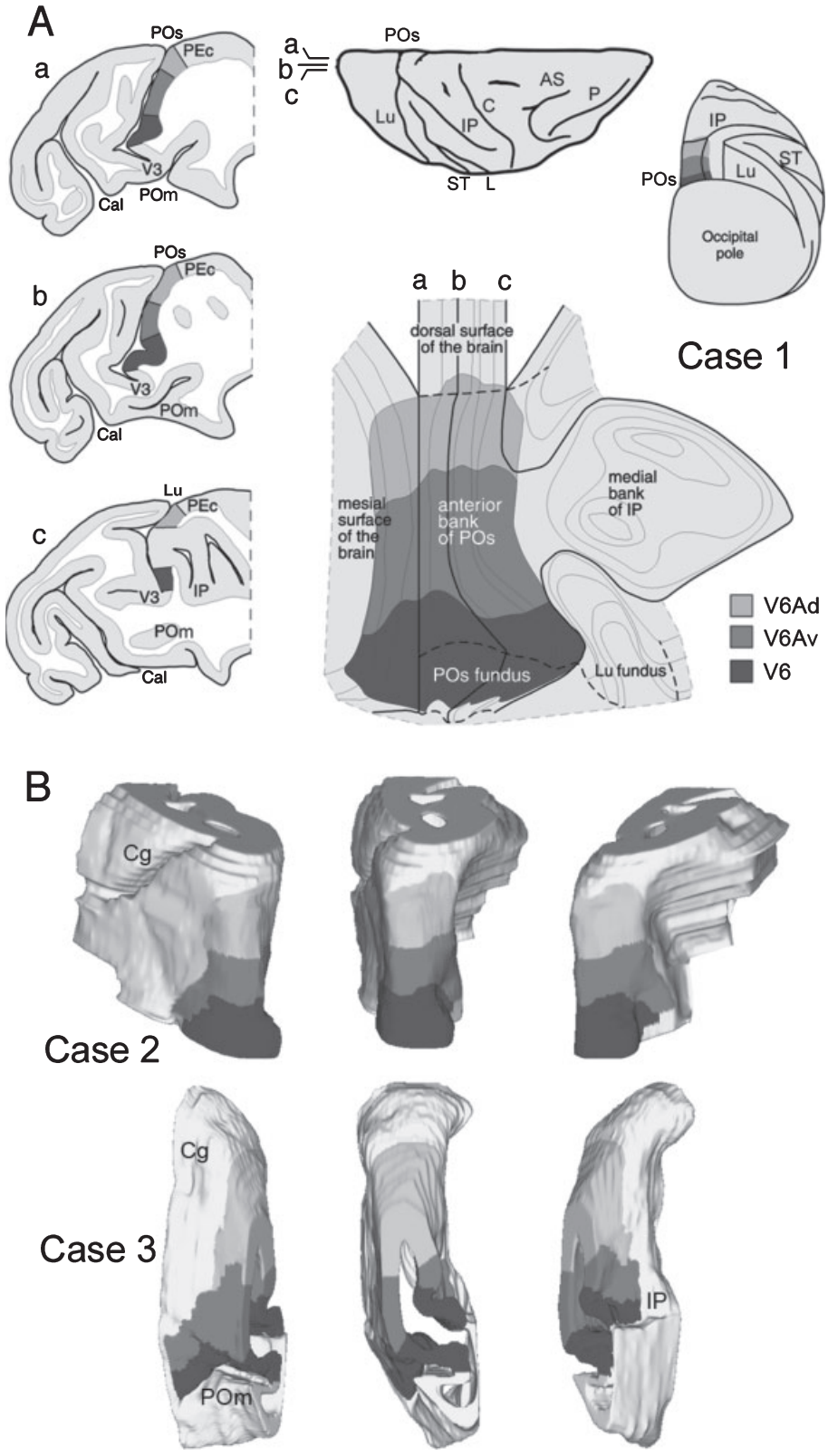

FIG. 10. Location and extent of anterior parieto-occipital areas V6, V6Av and V6Ad. (A) 2D reconstruction of the caudalmost part of the superior parietal lobule, obtained from parasagittal sections of Case 1. For details on the unfolding procedure see Materials and methods. Each line in the reconstruction shows the layer 4 contour of individual sections spaced 400 μm apart. Thicker lines (a, b and c) show the layer 4 contours of the three representative sections shown in left part of the figure. The approximate level at which the three sections were taken is indicated in the drawing of the dorsal view of the hemisphere. (B) 3D reconstructions of the caudalmost part of the superior parietal lobule obtained from horizontal sections of Case 2 (spaced 400 μm apart), and from coronal sections of Case 3 (spaced 300 μm apart). Dorsal is up and mesial is on the left. Each reconstruction is shown, from left to right, in a caudo-mesial, caudal and caudo-lateral view, respectively.

Brain location and extent of areas V6, V6Av and V6Ad

In order to reconstruct the brain location and extent of the three architectonic areas identified in this study, we used data from all three planes of sections, each of them being the most effective in showing data in specific parts of the SPL.

Figure 10 shows the location and extent of the architectonic areas V6, V6Av, and V6Ad in three representative hemispheres. Note that, in spite of the individual variability, the areal distribution is remarkably constant in different cases. A similar areal distribution was also observed in the remaining hemispheres of this study.

The flattened map shown in Fig. 10A was obtained according to the same procedures adopted in previous electrophysiological studies by Galletti and coworkers (see Materials and methods), and can therefore be used for comparing the location of cyto-architectonic areas with the distribution of functional properties of neurons recorded in the same cortical sector (see Galletti *et al.*, 1996, 1999a, 1999b). Figure 10B shows 3D reconstructions of the caudal part of the SPL of two hemispheres, one cut horizontally (Case 2), the other coronally (Case 3). Each hemisphere is shown from different views to see either the mesial cortical surface or the medial bank of the intraparietal sulcus. In the case cut coronally, the caudalmost sections were not included in the reconstruction because they were too tangential with respect to the cortical surface, and therefore not suitable for the definition of cytoarchitectonic areas. However, despite these limitations, and because the coronal is

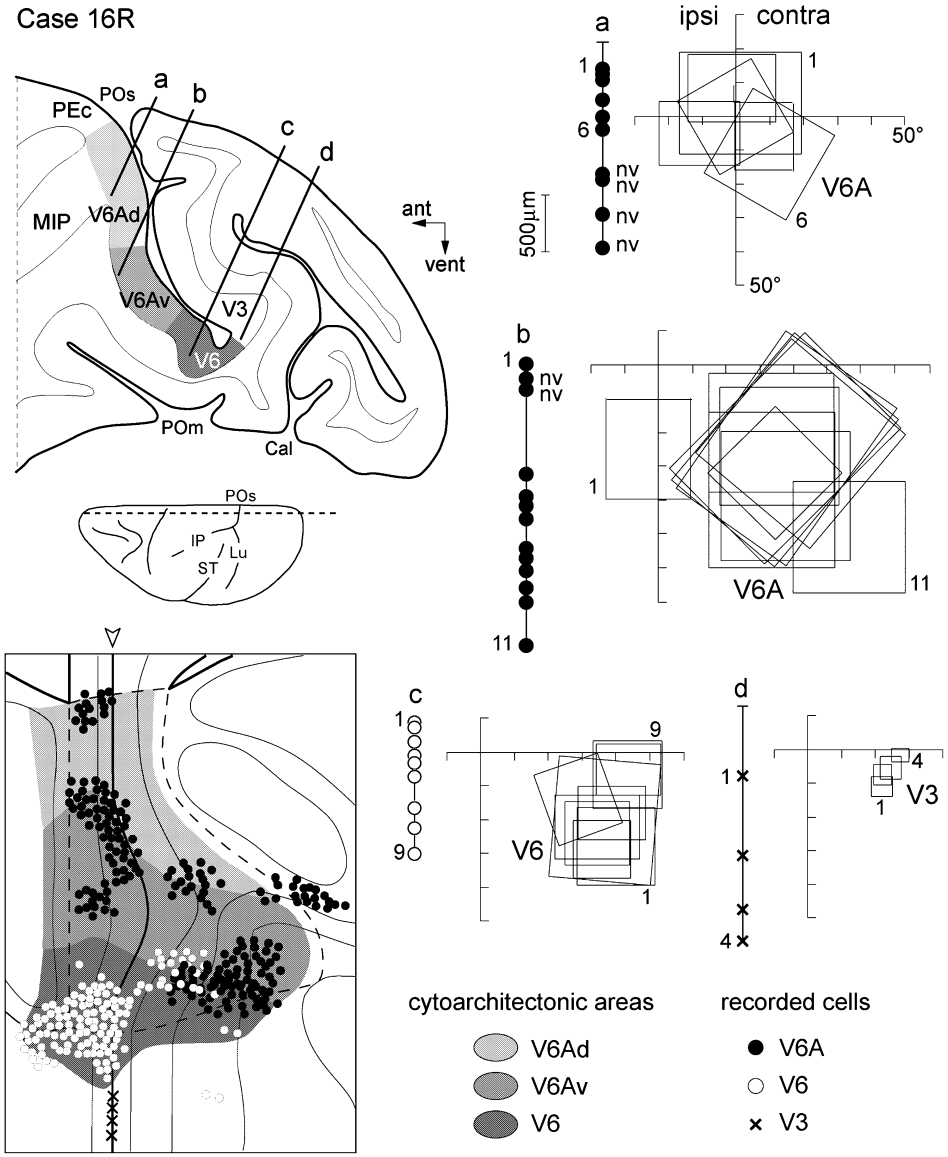

FIG. 11. Relationship between cytoarchitectonic and functional parcellation of the anterior wall of POs in a case which underwent chronic single unit recordings in the awake animal. (Top-left) Parasagittal section of the brain of Case MEF16R taken at the level shown on the brain silhouette. Four reconstructed microelectrode penetrations are shown on the section. Two penetrations (a and b) reached area V6A, one (c) area V6 and one (d) area V3. The grey sectors represent the three cytoarchitectonic subdivisions (V6, V6Av, V6Ad) of the anterior bank of POs according to the criteria described in this study. (Right) Insets showing the cell's type, receptive field, and recording depth along each penetration. Visual cells are numbered progressively along each penetration track; first and last numbers only are reported. Cells insensitive to visual stimulation are indicated as 'nv' (nonvisual). (Bottom-left) Distribution of cells functionally defined as V6 and V6A on a two-dimensional map of the caudalmost part of the superior parietal lobule in Case MEF16R. The three grey sectors represent the cytoarchitectonically defined areas V6, V6Av, and V6Ad. The arrowhead indicates the section shown on the top, and the dashed contour outlines the anterior bank of the POs.

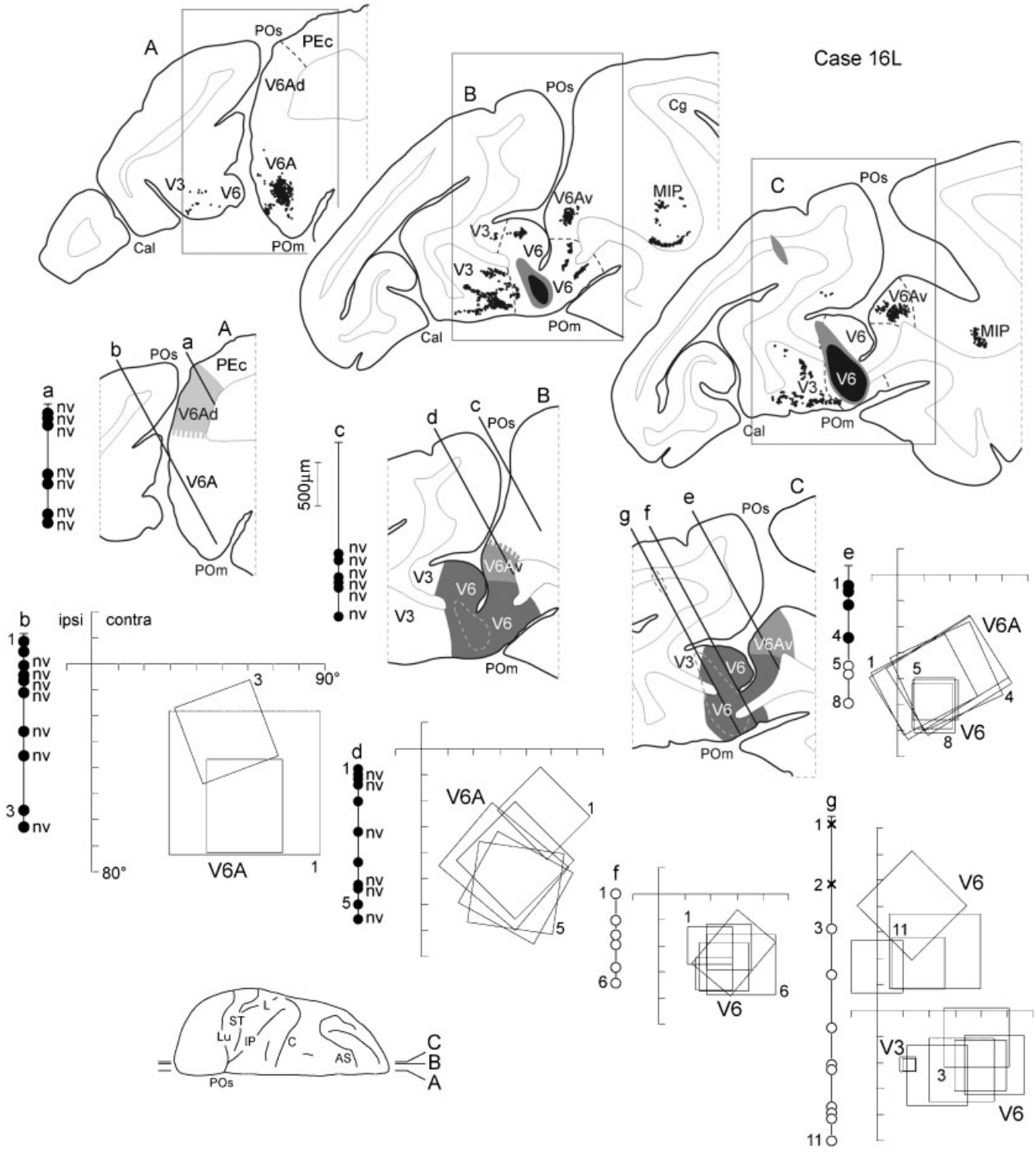

FIG. 12. Relationship between cytoarchitectural, functional parcellation and anatomical connections in a case that underwent chronic single unit recordings in the awake animal. (Top) Parasagittal sections taken at the level shown on the brain silhouette reported on the bottom part of the figure, showing the cortical distribution of retrogradely labelled cells after V6 injection of WGA-HRP in Case MEF16L. The core zone of the injection site is depicted in black, the halo zone in grey. Each dot on the sections represents a single labelled cell. Dashed lines through the grey matter of sections indicate the cytoarchitectonically defined borders between areas V3, V6, V6Av, V6Ad, and PEc. (Middle) Boxed areas in A, B, C in the top part of the figure are here shown together with the reconstruction of seven microelectrode penetrations. The grey sectors represent the cytoarchitectonic subdivisions of the anterior bank of POs according to the criteria described in this study. Dashed white lines delimitate the injection site, as shown in the upper part of the figure. Four penetrations (a, b, c and d) reached area V6A, one (e) both areas V6A and V6, one (f) only area V6, and one (g) both areas V3 and V6. (Bottom) Cell's type, receptive field, and recording depth for each penetration. Symbols and other details are as in Fig. 10.

the most widely used plan of cutting, we believe that this latter reconstruction can be useful for other laboratories to recognize locations of V6, V6Av, and V6Ad.

The 2D and 3D reconstructions of Fig. 10 thoroughly describe the brain location and extent of V6, V6Av and V6Ad, as well as their relationships with neighbouring cortical areas. Three points are worth noting. (i) V6Ad is mainly confined to the anterior wall of the POs, slightly extending over the mesial cortical surface and the medial bank of the intraparietal sulcus. Its dorsal border is close to the junction between the anterior bank of the POs and the exposed dorsal surface of SPL. (ii) V6Av extends more rostrally than V6Ad, both in the medial and lateral aspects of caudal SPL. V6Av completely surrounds anteriorly, medially, and laterally area V6. (iii) V6 is confined to the deepest part of the wall. It continues medially into the caudal, ventral tip of the precuneate cortex, often extending into the dorsal bank of the medial parieto-occipital sulcus (see Case 3). Laterally, V6 involves the fundus of the POs, as well as the ventral region of the most lateral part of the posterior bank of POs. This latter point is not always recognizable on the basis of architectural criteria because of the complex convolution of this region of the brain that makes it difficult to cut the cortex perpendicularly. However, it has always been observed during chronic recordings (Galletti *et al*., 1996, 1999a, 1999b), and in some cases, as in that shown in Fig. 12, it can also be demonstrated by architectural criteria.

Correlation of architectonic data with functional and connectional data

To confirm that the two main architectonic areas identified in the present study, V6 and V6A indeed correspond, as suggested by their location and extent, to the two functional areas V6 and V6A as defined by Galletti *et al*. (1996, 1999a, 1999b), a detailed cytoarchitectural study was carried out on two cases (MEF16, and MEF17; four hemispheres) that underwent chronic single unit recording in awake animals. Figure 11 shows an example of this study.

In the parasagittal section shown in the upper left part of Fig. 11, reconstructions of the trajectories of four electrode penetrations carried out at different dorso-ventral levels of the anterior wall of the POs are reported, along with the location and extents of cytoarchitectonic areas V6, V6Av, and V6Ad (depicted as dark, intermediate and light grey cortical sectors, respectively). The right part of the figure shows the size, topography and sequence of visual receptive fields of the neurons recorded in each penetration, together with the relative depth of recording sites along the anterior bank of POs. In the two more dorsal penetrations (a and b) nearby recorded cells presented large visual receptive fields, located in different parts of the visual field. Furthermore, a number of cells in each of these two penetrations (labelled nv in the figure) turned out to be insensitive to the visual stimulation. According to the criteria described by Galletti *et al*.

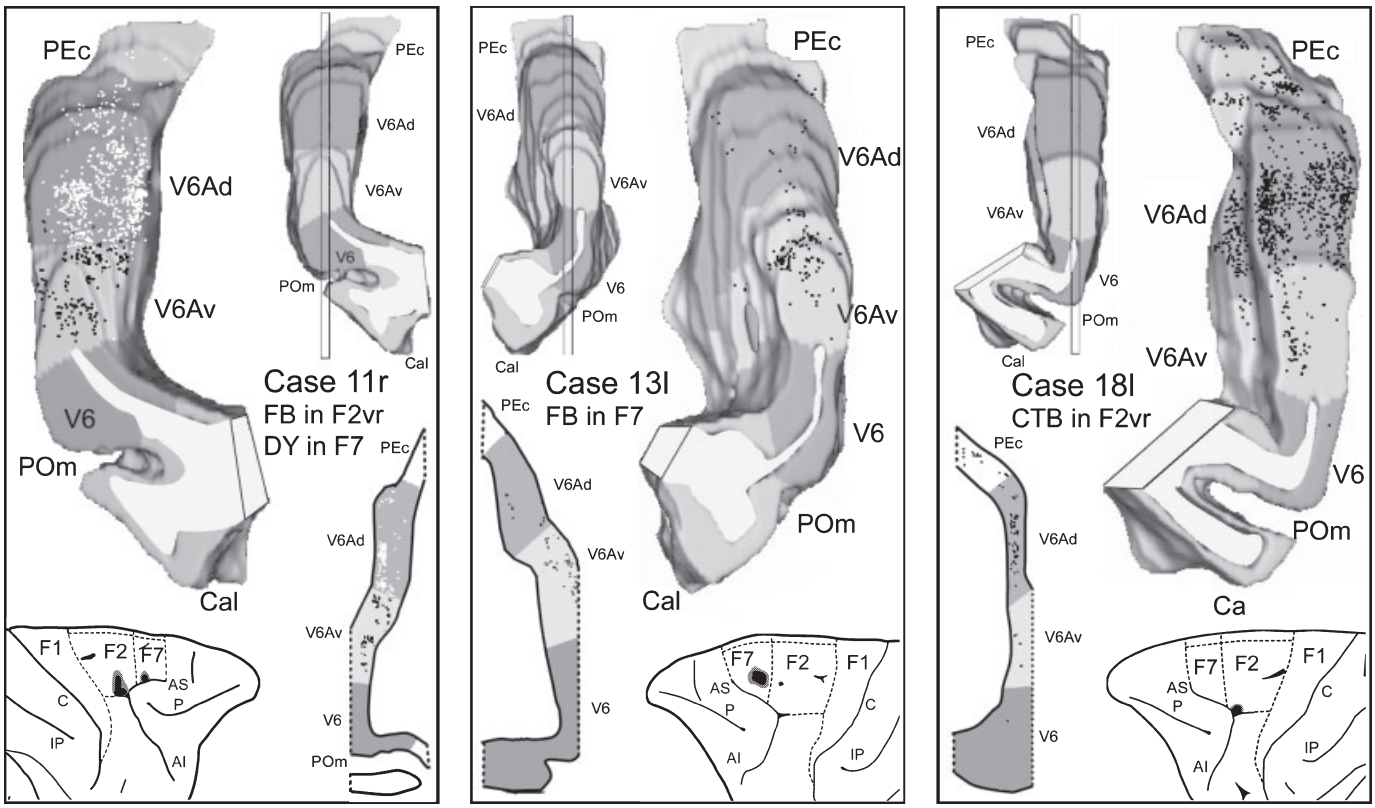

FIG. 13. Frontal projections from areas V6Av and V6Ad to dorsal premotor areas F7 and F2. The three panels in the figure show the distribution of retrogradely labelled neurons observed in the anterior wall of the POs following injections in F7 and ventrorostral F2 (left), in F7 (middle) and in ventrorostral F2 (right). In each panel, the distribution of marked neurons and the cytoarchitectonic borders of areas V6, V6Av and V6Ad are shown on a caudo-lateral and a caudal view of 3D reconstructions of the caudal SPL, and on a representative parasagittal re-slicing (600 μm thickness) from the 3D reconstruction. In the left panel, FB-labelled neurons and DY-labelled neurons are shown as white and black dots, respectively. The mediolateral level at which the parasagittal re-slicing was obtained is indicated by a box in the caudal view of the SPL. In each panel, drawings of a dorsolateral view of the frontal lobe show the location of the injection sites. In each drawing, dashed lines mark the cytoarchitectonic borders of areas F1 (area 4), F2 and F7.

(1996, 1999a), all these cells were assigned to the functional area V6A. The reconstruction shown in Fig. 11 demonstrates that all of them were located within the limits of the cytoarchitectonic area V6A.

In a more ventral penetration (penetration c), neurons recorded in the anterior bank of POs presented smaller visual receptive fields, which progressively shifted from the lower field representation to the horizontal meridian representation moving downward along the penetration. According to the criteria described by Galletti *et al*. (1996, 1999b), they were assigned to the functional area V6. The architectonic reconstruction showed that all of them were located within the limits of the cytoarchitectonic area V6.

Penetration d in Fig. 11 reached the posterior part of the fundus of POs, a cortical region located just behind that explored by penetration c. In penetration d, the receptive fields were much smaller than those encountered in penetration c. For size and topography, they were typical of area V3. The architectonic reconstruction confirmed that they were located in an occipital area different from V6, namely in V3.

The 2D reconstruction in the bottom left part of Fig. 11 shows the overall distribution of recorded cells in Case 16R, together with the location and extent of the cytoarchitectonically defined areas V6, V6Av, and V6Ad. It is evident that V6 cells (empty circles) and V6A cells (filled circles) matched quite well with the architectonic data. Almost all V6 neurons were confined within the limits of the cytoarchitectonic area V6, as well as V6A neurons were mainly located within the limits of the cytoarchitectonic area V6A. These data strongly suggest that the two main architectonic areas identified in the present study represent, with a high degree of confidence, the architectonic counterparts of the functional areas V6 and V6A.

On the basis of the examined visual receptive fields properties (size and retinotopy), no differences were observed between the dorsal and the ventral subdivisions of area V6A. However, the correlation of architectonic data with connectional data showed that architectonic areas V6Av and V6Ad have markedly different cortical connections. The upper part of Fig. 12 shows three representative parasagittal sections of Case MEF16, in which an injection of WGA-HRP was placed in the physiologically identified area V6 (Galletti *et al*., 2001). Cytoarchitectonic analysis showed that retrograde and anterograde labelling, originally assigned to area V6A, is strictly confined to architectonic area V6Av, whereas V6Ad does not appear to be directly connected with area V6 (compare the location of labelling in the upper part of Fig. 12 with the location of cytoarchitectonically defined areas V6, V6Av, and V6Ad shown in the bottom part of Fig. 12).

The bottom part of Fig. 12 also shows the type of cells encountered in the cortical regions cytoarchitectonically defined as V6, V6Av, and V6Ad. Here again, as in Fig. 11, there is a good match between the cell's functional properties and the architectonic classification. In turn, functional data shown in the bottom part of Fig. 12 confirm that V6 is connected with the ventral part of the functionally defined area V6A, but not with the dorsal part of it.

A further example of the difference in cortical connections between areas V6Av and V6Ad is presented in Fig. 13, which shows the distribution of the retrograde labelling in V6Av and V6Ad, observed following injections in the two dorsal premotor areas F2vr and F7, in three different monkeys (for further details, see Matelli *et al*., 1998). The analysis of Case 11r, showed that F2vr- and F7-projecting neurons (white and black dots, respectively) had a markedly different distribution in the anterior wall of the POs. This differential distribution, originally attributed to a possible topographic arrangement of the cortical connections of V6A, now clearly appears to be the result of a differential pattern of connectivity of architectonic areas V6Av and V6Ad. In particular, V6Av appears to almost exclusively project to F7, whereas V6Ad almost exclusively project to F2vr. The results obtained in Cases 18l and 13l are in agreement with those of Case 11r. In Case 13l, in which F7 was injected, labelled neurons were almost exclusively located in area V6Av; in Case 18l, where F2vr was injected, retrograde labelling was mostly confined to area V6Ad.

Discussion

Overview

The main aim of this study was to analyse the architectonic organization of the anterior wall of the POs in order to look for possible architectonic counterparts of the functionally defined areas V6 and V6A. Our results show that the anterior wall of POs contains at least two architectonic patterns, an occipital one ventrally, and a parietal one dorsally. These two patterns correspond very well to the extents and limits of the functionally defined areas V6 and V6A, respectively.

Moreover, the architectonically defined area V6A showed a nonhomogeneous cyto-, immuno-, and myeloarchitecture, so that it could be divided into a ventral (V6Av) and a dorsal (V6Ad) area. Correlation with hodological data showed that these two areas may correspond to hodologically distinct subdivisions, although no differences were observed on the basis of the basic receptive-fields properties (size and retinotopy) of the visual cells recorded in this cortical region. We cannot discard, however, the possibility that functional differences between V6Av and V6Ad could arise from the complex visual properties (see Galletti *et al*., 1996, 1999a), or extraretinal properties displayed by V6A cells, such as reach- and saccade-related activities (see Fattori *et al*., 2001; Kutz *et al*., 2003), as well as sensitivity to somatosensory stimulations (Breveglieri *et al*., 2002). More experiments are needed to clarify this point.

The present work represents the first detailed analysis of the cytoarchitecture of the caudalmost part of the SPL. It provides a tool for recognizing areas V6 and V6A in experiments lacking the functional markers needed to define areas V6 and V6A (see Galletti *et al*., 1996, 1999a, 1999b) and provides an anatomical frame of reference highly useful for the interpretation of functional and hodological data related to this region of the brain.

Architectonics of the anterior wall of the POs

The cytoarchitecture of the caudal part of the SPL was described in classic studies focused on the whole cerebral cortex (Brodmann, 1909; von Bonin & Bailey, 1947), as well as in more recent studies focused on the posterior parietal cortex (Pandya & Seltzer, 1982; Preuss & Goldmann-Rakic, 1991). In all these studies, the results are only available for the dorsolateral and mesial views of the hemisphere. In the study of Preuss & Goldmann-Rakic (1991), for instance, an area termed PO was defined on the mesial surface of the hemisphere, but no information was available on its extent within the POs. In the other three studies, as far as one can see from the published maps, it appears quite clear that the whole anterior wall of the POs was considered to belong to the occipital cortical domain (area 19 by Brodmann, 1909; area OA by von Bonin & Bailey, 1947; Pandya & Seltzer, 1982). It is evident therefore that there is a discrepancy between the previous studies and the present one, in which only the ventral third of the wall of the POs (area V6) is attributed to the occipital cortex.

Our criteria for the distinction between occipital and parietal cortical cytoarchitecture were based on cytoarchitectonic changes involving almost all the cortical layers. Actually, the general architectural

features described in the present study for the occipital areas (e.g. dense, well developed layer IV, dense and relatively homogeneous layer III, light layer V and very dense and outstanding layer VIb) and the parietal areas (well developed layer III with evident size gradient, well developed layer V with relatively large pyramids, less dense layer IV and a less sharp distinction of layer VI) are in substantial agreement with the description of areas OA and PE, respectively, by von Bonin & Bailey (1947), the only study in which detailed descriptions of the cytoarchitectonic areas in the caudal SPL are provided. In the present study, different planes of section were used in order to have optimal views of the cytoarchitecture of all the various parts of the caudal pole of the SPL, whereas in the studies of von Bonin & Bailey (1947) and Pandya & Seltzer (1982) only coronal sections were used. When the caudal pole of the SPL is cut coronally, the anterior wall of the sulcus is cut tangentially or very obliquely, and therefore its cytoarchitecture is particularly difficult to analyse. This difficulty was pointed out by von Bonin & Bailey (1947). In their analysis of individual sections, these authors described the architectonic pattern of the anterior bank of the POs as being basically of occipital type (area OA), though they noted that the upper part of the anterior wall of the POs had transitional characteristics, and defined this cortical sector as PEO. Given the uncertainties in locating cytoarchitectural borders on the anterior wall of the POs in coronal sections, it is possible that von Bonin & Bailey (1947) and Pandya & Seltzer (1982) settled the dorsal border of area OA more dorsally than its actual location.

Another approach used to define the architectonic organization of the caudal pole of the SPL is myeloarchitecture. By using a change in myelin density as major criterion, Colby *et al*. (1988) set the dorsal border of a strongly myelinated area, called PO, at approximately half of the anterior wall of the POs. In our myelin preparations, we confirmed the dorso-ventral change in myelination, but we identified, in the lower part of the wall, two myeloarchitectural changes that appear to correspond to the cytoarchitectonic borders between V6 and V6Av and between V6Av and V6Ad, respectively. The comparison of our data (e.g. Fig. 7) with those of Colby and coworkers (see, e.g. Fig. 2 of Colby *et al*., 1988) leads to the conclusion that area PO probably corresponds to V6 plus V6Av, with the ventral and dorsal borders of PO corresponding to the V3/V6 and V6Av/V6Ad borders, respectively. This implies that area PO, as defined by Colby *et al*. (1988), would include an occipital (V6) and a parietal (V6Av) area. This observation has important implications for the interpretation of functional and hodological data related to this region of the brain and will be discussed below.

The myeloarchitectural change we observed at the V6/V6Av border was not reported in the study of Colby *et al*. (1988), possibly because it was hidden within the more myelinated region of the anterior bank of the POs. Actually, V6Av is well myelinated, though less than V6. Thick vertical bundles of fibers are present also in V6Av, though sparser than in V6, and both Baillarger bands are clearly visible. The presence of vertical bundles of fibres and of both bands of Baillarger give to V6Av a myelinated dark aspect and were considered as typical features of area PO. This could account for the fact that the V6/V6Av border was not identified, and that the dorsal border of area PO was placed at the level of V6Av/V6Ad border.

In a recent study, Lewis & Van Essen (2000) described an area PO characterized by heavy myelination and strong radial component of myelinated fibres and strong SMI-32 immunoreactivity in layer III. This study was mostly based on the analysis of coronal sections where, as described above, it is difficult to appreciate the exact location of architectural borders in the anterior wall of the POs. In addition, the study reported only the core of PO architectonic subdivision, so that its extent did not represent the full extent of PO. For these reasons, it is difficult to compare the results of Lewis & Van Essen (2000) with those of Colby *et al*. (1988), and with those reported in the present study. In any case, it appears that the location and extent of the area PO reported by the above-mentioned authors are similar one to the other, but different from that of the present study, leaving unchanged our suggestion that area PO includes both areas V6 and V6Av.

Also in the study of Hof & Morrison (1995), which characterized visual areas of the occipital, parietal and temporal cortex on the basis of different patterns of regional distribution of SMI-32 immunoreactivity, the presented material is from coronal sections and no maps of the identified areas were provided. In this study, however, area PO was distinguished by densely packed intermediate-sized SMI-32 immunoreactive pyramids in layer IIIc, displaying long, thin apical dendrites ascending up to superficial layers, a description that appears to closely fit with our observation on distribution of SMI-32 immunoreactivity in area V6. Furthermore, similarly to our observations, parietal areas bordering PO, defined as MIP, laterally and MDP, medially, were distinguished by lesser layer III immunoreactivity and a higher number of layer V positive neurons. In spite of these similar observations, in a low-power photomicrograph of a coronal section shown in their Fig. 1, Hof & Morrison (1995) attributed the anterior wall of POs almost entirely to area PO. Although any judgement on a single section must be taken with caution, especially if at a very low-power view, we note that in the section shown by Hof & Morrison (1995), the labelling in layer V becomes higher at a level dorsal to the POm, both on the mesial and lateral aspect of the SPL. This could correspond to the level of the V6/V6Av border defined in our study.

Correlation with functional and hodological data

Single unit recording studies of the anterior bank of POs showed that V6 is a retinotopically organized visual area with a complete representation of the contralateral visual hemifield (Galletti *et al*., 1999b). V6A, in contrast, contains visual neurons with larger receptive fields not retinotopically organized (Galletti *et al*., 1999a), and contains also approximately 40% of neurons insensitive to the visual stimulation, many of which are sensitive to somatosensory stimulation (Breveglieri *et al*., 2002) and/or to the execution of arm movements (Galletti *et al*., 1997; Fattori *et al*., 2001). The comparison between the cytoarchitectonic subdivision proposed in the present study and the functional subdivision of the same cortical region proposed by Galletti *et al*. (1996, 1999a, 1999b) strongly suggest that the functionally defined areas V6 and V6A have cyto-, immuno-, and myeloarchitectural counterparts. This has been proven here in cases where both single unit recordings and cytoarchitectural studies were carried out. According to these data, V6 is an occipital area, with a retinotopic organization similar to that of the other occipital extrastriate areas. Area V6 appears to be the origin of a relatively direct visuo-motor pathway (dorso-medial stream of Galletti *et al*., 2003; dorso-dorsal stream of Rizzolatti & Matelli, 2003) that reaches, in a few cortical steps, the arm-related fields of the PMd (see Galletti *et al*., 2003; Rizzolatti & Matelli, 2003).

Recent tract tracing data have shown that V6 is target of strong projections from V1 and is connected with several extrastriate and posterior parietal areas, but has no connections with any area of the frontal lobe (Galletti *et al*., 2001). In contrast, several studies (Matelli *et al*., 1998; Shipp *et al*., 1998; Galletti *et al*., 2001; Marconi *et al*., 2001) have shown that V6A does not receive from V1 and is strongly connected with the posterior parietal areas 7a and PGm (which are not connected to V6) and with the caudal (F2) and rostral (F7) PMd areas

of the frontal lobe. As suggested by the present data, area PO of Colby *et al*. (1988) likely includes the occipital area V6 plus the parietal area V6Av. This could explain why PO, but not V6, is connected with areas 7a and PGm (due to the possible involvement of the ventral part of V6A by the injection site). Our view also explains why a tracer injection in PMd labels only the dorsal part of PO (Tanné *et al*., 1995), namely the ventral part of V6A.

The present results also show hodological evidence in favour of a dorso-ventral distinction within area V6A. In particular (i) V6Av, but not V6Ad, is directly connected with V6 (independently from the location of the injection site in V6) and (ii) V6Av and V6Ad mostly project to two hodologically and functionally distinct premotor areas, F7 and F2vr, respectively (Matelli *et al*., 1998; Luppino *et al*., 2003).

Additional functional findings reported in the literature suggest the existence of a dorso-ventral segregation within area V6A. For instance, nonvisual neurons activated by somatosensory stimuli or by the execution of arm movements appear to be more present in the dorsal part of V6A, while the ventral part of V6A shows a higher sensitivity to the visual stimulation (Fattori *et al*., 1999). In addition, the ventral part of V6A, but not the dorsal one, contains cells able to directly encode the visual space (Galletti *et al*., 1999a).

In conclusion, the hypothesis that area V6A is subdivided in a ventral (V6Av) and dorsal (V6Ad) area seems to be reliable, being suggested by cytoarchitectural, hodological as well as functional criteria. The present data appear to provide a firm anatomical frame of reference for the interpretation and guidance of future functional and hodological studies focused on this cortical region.

Acknowledgements

Professor Massimo Matelli died on August 2003. The authors are profoundly indebted to him for his contribution in the data analysis and the preliminary preparation of this manuscript and agreed that his name had to be included as a coauthor in this manuscript. We wish to remember him not only as a scientist, but also as a person contagious in his enthusiasm for research and as an example for all of us. The 3D-reconstruction software was developed by CRS4, Pula, Cagliari, Italy. S.B.H was supported by a fellowship from the Fyssen Foundation. This study was supported by MIUR.

Abbreviations

PMd, dorsal premotor cortex; POm, medial parieto-occipital sulcus; POs, parieto-occipital sulcus; SPL, superior parietal lobule.

References

Ben Hamed, S., Luppino, G. & Matelli, M. (2000) Architectonic definition of the mesial parietal cortex and of the adjacent mesial areas in the macaque. *Soc. Neurosci. Abstr.*, 249.241.

Bettio, F., Demelio, S., Gobbetti, E., Luppino, G. & Matelli, M. (2001) Interactive 3-D reconstruction and visualization of primates cerebral cortex. *Soc. Neurosci. Abstr.*, 728.724.

von Bonin, G.& Bailey, P. (1947) *The Neocortex of Macaca Mulatta*. University of Illinois Press, Urbana.

Breveglieri, R., Kutz, D.F., Fattori, P., Gamberini, M. & Galletti, C. (2002) Somatosensory cells in the parieto-occipital area V6A of the macaque. *Neuroreport*, **13**, 2113–2116.

Brodmann, K. (1909) *Vergleichende Lokalisationslehre der Grosshirnrinde*, Barth, Leipzig. (Reprinted 1925).

Calzavara, R., Zappalà, A., Rozzi, S., Matelli, M. & Luppino, G. (2005) Neurochemical characterization of the cerebellar-recipient motor thalamic territory in the macaque monkey. *Eur. J. Neurosci.*, **21**, 1869–1894.

Campbell, M.J. & Morrison, J.H. (1989) Monoclonal antibody to neurofilament protein (SMI-32) labels a subpopulation of pyramidal neurons in the human and monkey neocortex. *J. Comp. Neurol.*, **282**, 191–205.

Carmichael, S.T. & Price, J.L. (1994) Architectonic subdivision of the orbital and medial prefrontal cortex in the macaque monkey. *J. Comp. Neurol.*, **346**, 366–402.

Colby, C.L. & Duhamel, J.-R. (1991) Heterogeneity of extrastriate visual areas and multiple parietal areas in the macaque monkeys. *Neuropsychologia*, **29**, 517–537.

Colby, C.L., Gattass, R., Olson, C.R. & Gross, C.G. (1988) Topographical organization of cortical afferents to extrastriate visual area PO in the macaque: a dual tracer study. *J. Comp. Neurol.*, **269**, 392–413.

Covey, E., Gattass, R. & Gross, C.G. (1982) A new visual area in the parieto-occipital sulcus of the macaque. *Soc. Neurosci. Abstr.*, **8**, 681.

Cusick, C.G., Seltzer, B., Cola, M. & Griggs, E. (1995) Chemoarchitectonics and corticocortical terminations within the superior temporal sulcus of the rhesus monkey: evidence for subdivisions of superior temporal polysensory cortex. *J. Comp. Neurol.*, **360**, 513–535.

Demelio, S., Bettio, F., Gobbetti, E. & Luppino, G. (2001) Three-dimensional reconstruction and visualization of the cerebral cortex in primates. In Ebert, D., Favre, J. & Peikert, R., (Eds), *Data Visualization. 2001.* (Proceedings of the Joint Eurographics and IEEE TCVG Symposium on Visualization, Ascona, Switzerland, May 28–30, 2001).

Fattori, P., Gamberini, M., Kutz, D.F. & Galletti, C. (2001) 'Arm-reaching' neurons in the parietal area V6A of the macaque monkey. *Eur. J. Neurosci.*, **13**, 2309–2313.

Fattori, P., Gamberini, M., Mussio, A., Breveglieri, R., Kutz, D.F. & Galletti, C. (1999) A visual-to-motor gradient within area V6A of the monkey parieto-occipital cortex. *Neurosci. Lett. Supplement*, **52**, S22.

Galletti, C., Fattori, P., Battaglini, P.P., Shipp, S. & Zeki, S. (1996) Functional demarcation of a border between areas V6 abd V6A in the superior parietal gyrus of the macaque monkey. *Eur. J. Neurosci.*, **8**, 30–52.

Galletti, C., Fattori, P., Gamberini, M. & Kutz, D.F. (1999b) The cortical visual area V6: brain location and visual topography. *Eur. J. Neurosci.*, **11**, 3922–3936.

Galletti, C., Fattori, P., Kutz, D.F. & Battaglini, P.P. (1997) Arm movement-related neurons in visual area V6A of the macaque superior parietal lobule. *Eur. J. Neurosci.*, **9**, 410–413.

Galletti, C., Fattori, P., Kutz, D.F. & Gamberini, M. (1999a) Brain location and visual topography of cortical area V6A in the macaque monkey. *Eur. J. Neurosci.*, **11**, 575–582.

Galletti, C., Gamberini, M., Kutz, D.F., Fattori, P., Luppino, G. & Matelli, M. (2001) The cortical connections of area V6: an occipito-parietal network processing visual information. *Eur. J. Neurosci.*, **13**, 1572–1588.

Galletti, C., Kutz, D.F., Gamberini, M., Breveglieri, R. & Fattori, P. (2003) Role of the medial parieto-occipital cortex in the control of reaching and grasping movements. *Exp. Brain Res.*, **153**, 158–170.

Gallyas, F. (1979) Silver staining of myelin by means of physical development. *Neurol. Res.*, **1**, 203–209.

Gamberini, M., Galletti, C., Luppino, G. & Matelli, M. (2002) Cytoarchitectonic organization of the functionally defined areas V6 and V6A in the parieto-occipital cortex of macaque brain. *J. Physiol. (Lond.)*, **543**, 113P.

Gattass, R., Sousa, A.P.B. & Cowey, E. (1985) Cortical visual areas of the macaque. Possible Substrates for Pattern Recognition Mechanisms. In Ghagas, C., Gattass, R. & Gross, C.G., (Eds), *Pattern recognition mechanisms.* Pontifical Academy of Sciences, Vatican City, pp. 1–20.

Geyer, S., Matelli, M., Luppino, G. & Zilles, K. (2000) Neurofilament protein distribution in the macaque monkey dorsolateral premotor cortex. *Eur. J. Neurosci.*, **12**, 1554–1566.

Hof, P.R. & Morrison, J.H. (1995) Neurofilament protein defines regional patterns of cortical organization in the macaque monkey visual system: a quantitative immunohistochemical analysis. *J. Comp. Neurol.*, **352**, 161–186.

Kutz, D.F., Fattori, P., Gamberini, M., Breveglieri, R. & Galletti, C. (2003) Early- and late-responding cells to saccadic eye movements in the cortical area V6A of macaque monkey. *Exp. Brain Res.*, **149**, 83–95.

Lewis, J.W. & Van Essen, D.C. (2000) Mapping of architectonic subdivisions in the macaque monkey, with emphasis on parieto-occipital cortex. *J. Comp. Neurol.*, **428**, 79–111.

Luppino, G., Calzavara, R., Rozzi, S. & Matelli, M. (2001) Projections from the superior agranular frontal cortex in the temporal sulcus to the macaque. *Eur. J. Neurosci.*, **14**, 1035–1040.

Luppino, G., Matelli, M., Gamberini, M. & Galletti, C. (2003) Cytoarchitectonic organization of the anterior bank of the parieto-occipital sulcus in macaque brain. *Soc. Neurosci. Abstr.*, **701**, 19.

Marconi, B., Genovesio, A., Battaglia Mayer, A., Ferraina, S., Squatrito, S., Molinari, M., Lacquaniti, F. & Caminiti, R. (2001) Eye-hand coordination during reaching. I. Anatomical relationships between parietal and frontal cortex. *Cereb. Cortex*, **11**, 513–527.

Matelli, M., Govoni, P., Galletti, C., Kutz, D.F. & Luppino, G. (1998) Superior area 6 afferents from the superior parietal lobule in the macaque monkey. *J. Comp. Neurol.*, **402**, 327–352.

Matelli, M. & Luppino, G. (2004) Architectonics of the primates cortex: usefulness and limits. *Cortex*, **40**, 209–210.

Nimchinsky, E.A., Hof, P.R., Young, W.G. & Morrison, J.H. (1996) Neurochemical, morphologic, and laminar characterization of cortical projection neurons in the cingulate motor areas of the macaque monkey. *J. Comp. Neurol.*, **374**, 136–160.

Pandya, D.N. & Seltzer, B. (1982) Intrinsic connections and architectonics of posterior parietal cortex in the rhesus monkey. *J. Comp. Neurol.*, **204**, 196–210.

Preuss, T.M. & Goldmann-Rakic, P.S. (1991) Myelo- and cytoarchitecture of the granular frontal cortex and surrounding regions in the strepsirhine primate *Galago* and the anthropoid primate *Macaca*. *J. Comp. Neurol.*, **310**, 429–474.

Rizzolatti, G. & Matelli, M. (2003) Two different streams form the dorsal visual stream: anatomy and functions. *Exp. Brain Res.*, **153**, 146–157.

Shipp, S., Blanton, M. & Zeki, S. (1998) A visuo-somatomotor pathway through superior parietal cortex in the macaque monkey: cortical connections of areas V6 and V6A. *Eur. J. Neurosci.*, **10**, 3171–3193.

Tanné, J., Boussaoud, D., Boyerzeller, N. & Rouiller, E.M. (1995) Direct visual pathways for reaching movements in the macaque monkey. *Neuroreport*, **7**, 267–272.

Van Essen, D.C. & Zeki, S. (1978) The topographic organization of rhesus monkey prestriate cortex. *J. Physiol. (Lond.)*, **277**, 193–226.

Zeki, S. (1986) The anatomy and physiology of area V6 of macaque visual cortex. *J. Physiol. (Lond.)*, **381**, 62P.